We are IntechOpen, the world's leading publisher of Open Access books Built by scientists, for scientists

4,800
Open access books available

122,000
International authors and editors

135M
Downloads

Our authors are among the

154
Countries delivered to

TOP 1%
most cited scientists

12.2%
Contributors from top 500 universities

CLARIVATE ANALYTICS BOOK CITATION INDEX INDEXED

WEB OF SCIENCE™

Selection of our books indexed in the Book Citation Index in Web of Science™ Core Collection (BKCI)

Interested in publishing with us?
Contact book.department@intechopen.com

Numbers displayed above are based on latest data collected.
For more information visit www.intechopen.com

Chapter 8

Nanofluid with Colloidal Magnetic Fe_3O_4 Nanoparticles and Its Applications in Electrical Engineering

Lucian Pîslaru-Dănescu, Gabriela Telipan, Floriana D. Stoian, Sorin Holotescu and Oana Maria Marinică

Additional information is available at the end of the chapter

http://dx.doi.org/10.5772/65556

Abstract

In this study, we propose a new type of a cooling agent based on magnetic nanofluid for the purpose of replacing the classical cooling fluids in electrical power transformers. The magnetite (Fe_3O_4) nanoparticles were synthesized by the co-precipitation method from an aqueous medium of salts $FeCl_3x6H_2O$ and $FeSO_4x7H_2O$ in the molar ratio Fe^{3+}/Fe^{2+} = 2:1, by alkalization with 10% aqueous solution of NaOH at 80°C, for 1 h. The size of the magnetite nanoparticles, as measured by X-ray diffraction method, was 14 nm and by scanning electron microscopy (SEM), they are between 10 and 30 nm. Magnetite powder was placed in oleic acid as a surfactant to prevent agglomeration of nanoparticles. The resulting mixture was dispersed in transformer oil UTR 40, with the role of carrier liquid. The magnetic, rheological, thermal and electrical characteristic properties of the obtained Fe_3O_4 transformer oil-based nanofluid were determined. A mathematical model and numerical simulation results are very useful for investigating the heat transfer performances of the magnetic nanofluid. Based on this study, it was tested the cooling performance of this magnetic nanofluid for two types of electrical power transformers as compared to classical methods. We also presented a microactuator based on the same magnetic nanofluid.

Keywords: colloidal magnetic Fe_3O_4 nanoparticles, X-ray diffraction, SEM, electrical transformer, magnetic nanofluid coolant, heat transfer, magnetic properties, microactuator, mass transfer, pulse width modulation, mathematical model, numerical simulation

1. Introduction

Magnetic nanofluids, known also as ferrofluids or magnetic liquids, are stable colloidal suspensions of superparamagnetic nanoparticles such as γ-Fe_2O_3, α-Fe_2O_3, Fe_3O_4, $CoFe_2O_4$,

$Mn_{1-x}Zn_xFe_2O_4$, in a carrier liquid (an organic solvent or water) [1–5]. In order to prevent the aggregation of magnetic nanoparticles and to attain a stable magnetic nanofluid, the nanoparticles are coated with a surfactant during the preparation process [1, 4–8]. The characterization of magnetic nanoparticles and of the obtained magnetic nanofluid is carried out by various techniques in order to determine their structural, magnetic, rheological and magneto-rheological properties [1–11]. The development of the synthesis methods leads to the possibility of tailoring the magnetic nanofluids and consequently, their physical properties, such that it fulfills the requirements of a certain application [1, 5, 12–24].

Besides the well-known application of ferrofluids in sealing and lubrication, recent developments envisaged their potential in fields like actuation [22, 23], medicine [1, 16], biotechnology [14, 24], as cooling fluids [25–29] or as liquid core in power transformers [30, 31]. The applications in medicine and biotechnology require from the magnetic nanofluid to be biocompatible. Therefore, water-based magnetic nanofluids are the candidates for magnetic hyperthermia for cancer treatment and targeted drug delivery, as well magnetic separation for purification of cells, proteins or else. The applications envisaged in electrical engineering require from the proposed magnetic nanofluid to also have good thermal and insulating properties. These conditions can be fulfilled by the transformer oil-based magnetic nanofluids.

This chapter is addressing the application of a Fe_3O_4 magnetic nanofluid based on transformer oil, as cooling and insulating fluid of a power transformer. Thus, the preparation procedure and the characterization of structural, magnetic, rheological, thermal and electrical properties are presented. The mathematical model applied to the problem is introduced, and the numerical results for two power transformers are discussed. The use of this Fe_3O_4 magnetic nanofluid in a micro-actuation application is also presented.

2. The synthesis and complex characterization of nanofluid with colloidal magnetic Fe_3O_4 nanoparticles

2.1. Nanofluid synthesis

The materials used for the synthesis of nanofluid with colloidal magnetic Fe_3O_4 nanoparticles we can mention: hexahydrated ferric chloride ($FeCl_3x6H_2O$) of 99% purity obtained from Merck Germany; ferrous sulfate sheptahydrate ($FeSO_4x7H_2O$) of 98% purity purchased from Chimopar, Romania; sodium hydroxide (NaOH) of 99% purity and oleic acid ($C_{18}H_{34}O_2$) of 99% purity provided by Riedel de Haen. Other chemicals were of analytic grade. The reagents were used without further purification. All solutions were prepared with deionized water.

The transformer oil-based ferrofluid with Fe_3O_4 nanoparticles was synthesized by chemical co-precipitation method [23], using $FeCl_3 \times 6H_2O$ and $FeSO_4 \times 7H_2O$ with a molar ratio of $Fe^{2+}/Fe^{3+} = 1:2$, dissolved in 300 ml of water and treated with NaOH 10%. The mixture was stirred at 80°C for 1 h. The resulting black color precipitate of Fe_3O_4 was washed with deionized water and magnetically decanted until a pH of 7 was reached. Then, 10 ml of HCl 0.1 N was added to the Fe_3O_4 precipitate for peptization. The mixture was washed and decanted again until pH 7, dried at 90°C and treated with acetone for water removal. A small part of the obtained powder

http://dx.doi.org/10.5772/65556

was analyzed [X-ray diffraction, scanning electron microscopy (SEM) and elemental analysis EDX] for structural properties. The remaining part of the powder was treated with 2 ml of oleic acid as surfactant, and with 5 ml of toluene and heated at 90°C for toluene removal. Finally, the mixture was dispersed in 50 ml of UTR 40 transformer oil, under strong stirring for 20 h in order to obtain the magnetic nanofluid. **Figure 1** schematically presents the transformer oil-based magnetic nanofluid of Fe_3O_4 synthesis.

2.2. Nanofluid characterization

2.2.1. Powder characterization of Fe_3O_4 nanoparticles

The Fe_3O_4 powder was structurally characterized by X-ray diffraction using a diffractometer D8 ADVANCE type X Bruker-AXS in conditions: Cu-Kα radiation (γ = 1.5406 Å), 40 KV/40 mA,

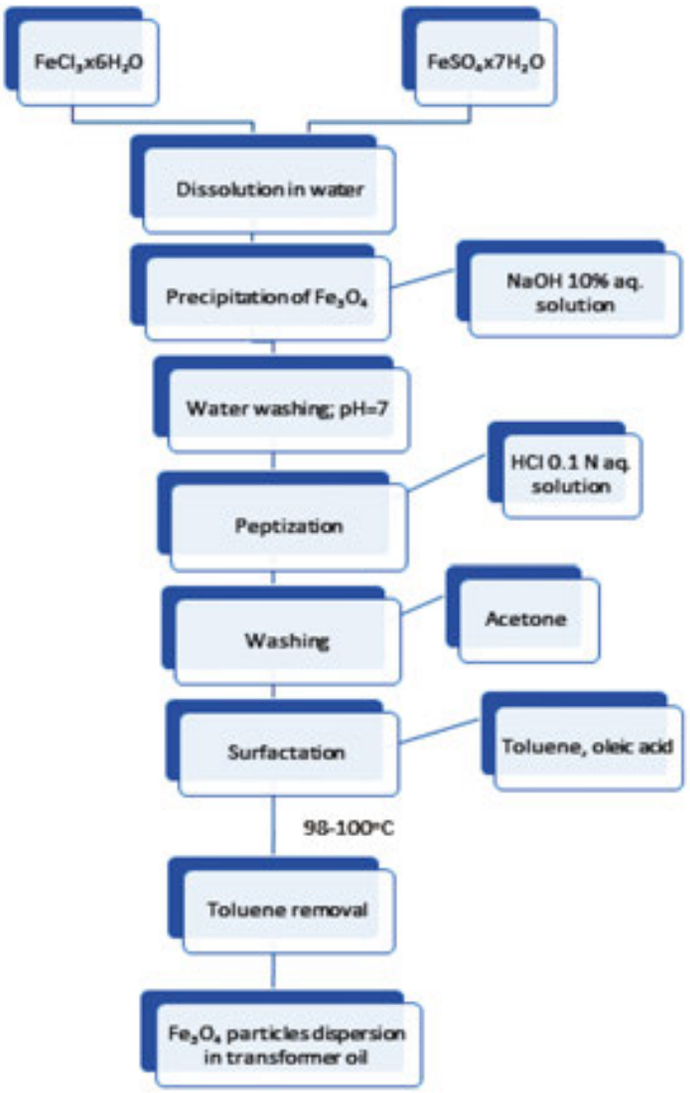

Figure 1. Transformer oil-based magnetic nanofluid of Fe_3O_4 synthesis.

filter k_β of Ni, in the 2θ range of 25–70°, using a step of 0.04° and measuring time on point of 1 s.

The XRD pattern of the powder is presented in **Figure 2** and shows the peaks corresponding to the Fe_3O_4 highlighted by "hkl" Miller indices (220), (311), (400), (422), (511) and (440), [2, 4], which denote a spinel structure with lattice parameter a = 0.83778 nm, in accord with the literature data (JCPDS file no. 19-629). According to the (311) peak, the medium size of the crystallites determined by Scherrer formula (1) is 14 nm.

$$D = \frac{0.9\lambda}{B^* \cos\theta}, \tag{1}$$

where D is the crystallites medium size, γ is the wavelength of this X-ray (γ = 0.154059 nm), B^* is the full width at half maximum (FWHM) and θ is the half diffraction angle of crystal orientation peak.

The morphology of the sample was studied by SEM using a Carl Zeiss SMT FESEM-FIB Auriger type scanner. The elemental analysis (energy-dispersive X-ray spectroscopy EDX) was performed with an energy dispersive probe of Inca Energy 250 type Oxford Instruments LTD England coupled to SEM.

The topology of the Fe_3O_4 powder analyzed by scanning electron microscopy evidenced two types of surface: smooth surface and rough surface (fracture). A crystalline structure of the material was found for the first type of surface, which is composed of crystallites having

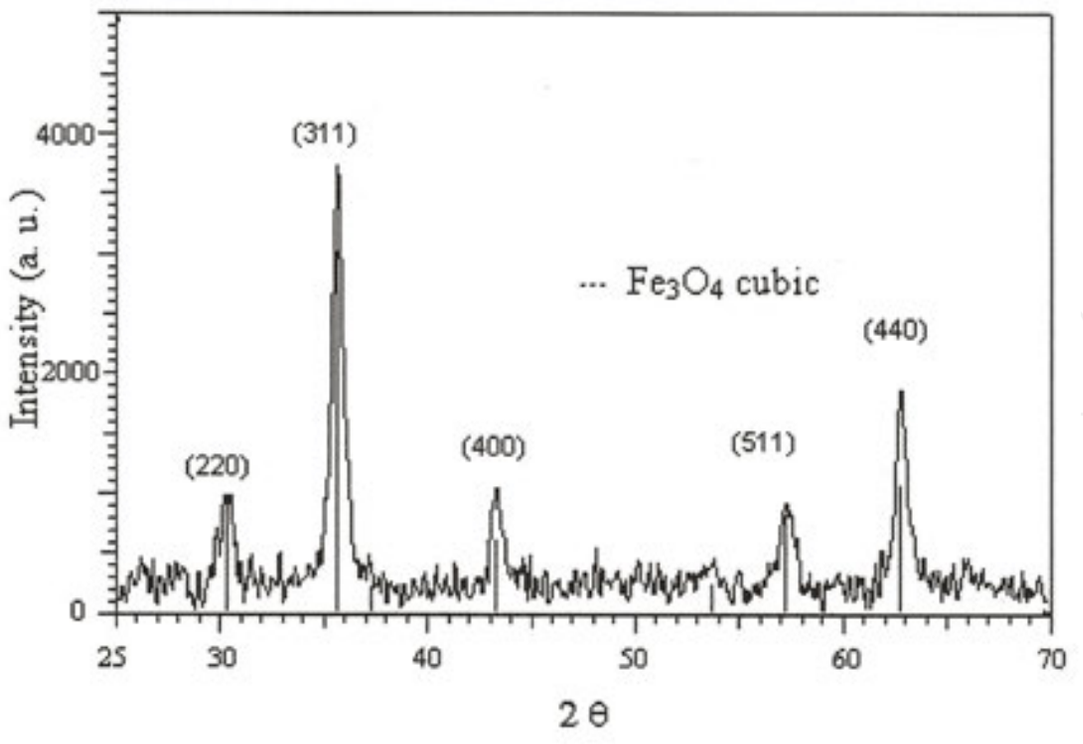

Figure 2. The Fe_3O_4 XRD pattern of the Fe_3O_4 nanoparticles.

average sizes between 10 and 30 nm (**Figure 3**) in good agreement with the diffraction analysis. For the second type of surface, a structure of acicular type agglomerates was found (**Figure 4**).

The elemental analysis confirms the presence of Fe_3O_4 (**Figure 5**) and shows that the resulting black powder contains 70.14%Fe, 24.96% O, 4.16% C and 0.74% Cl (**Table 1**). The presence of the Fe_3O_4 is exhibited by elemental Fe-peaks of about 6.45 and 0.75 keV. The high percentage of oxygen is related to its existence in the iron oxide.

The SEM image (**Figure 5a**) and the elemental energy dispersive X-ray analysis (**Figure 5b**) confirms the data determined by X-ray diffraction. The content of C and Cl represents the little impurities.

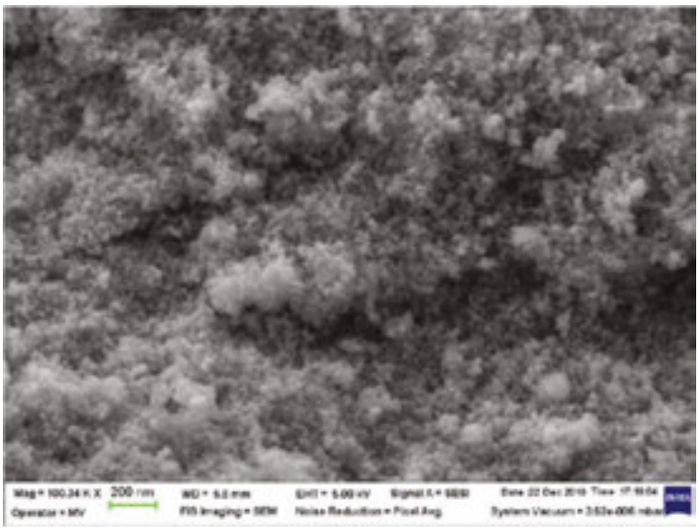

Figure 3. The SEM image for the first structure.

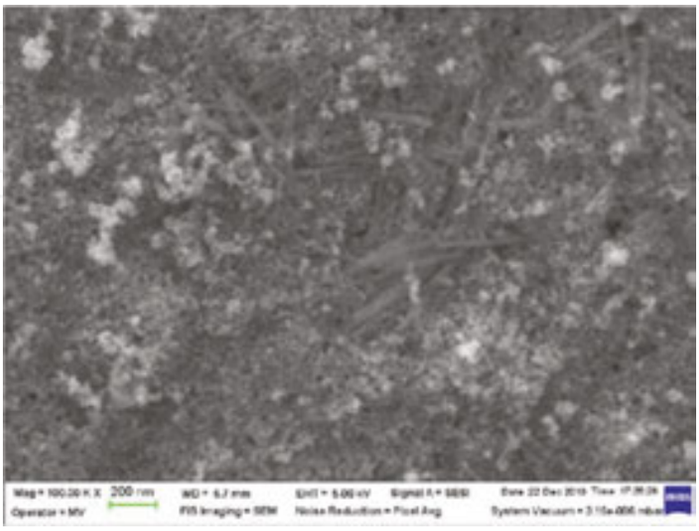

Figure 4. The SEM image for the second structure.

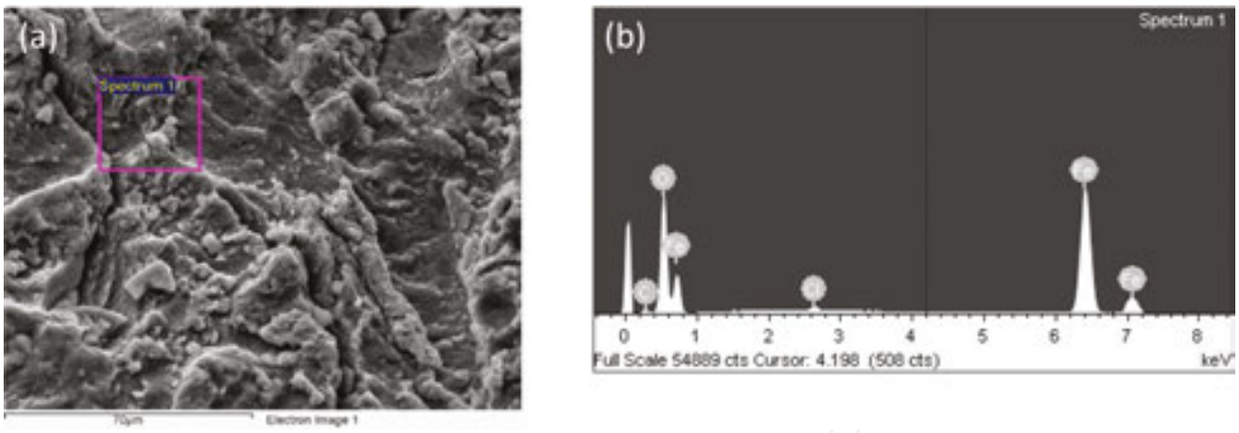

Figure 5. The elemental analysis for Fe_3O_4 powder: (a) the SEM image and (b) the elemental energy dispersive X-ray analysis.

Element	Weight (%)	Atomic (%)
C K	4.16	10.89
O K	24.96	49.01
Cl K	0.74	0.66
Fe K	70.14	39.45
Totals	100.00	100.00

Table 1. Analysis data for Fe_3O_4 nanoparticles, energy dispersive.

2.2.2. Characteristic properties of the nanofluid with colloidal magnetic Fe_3O_4 nanoparticles used as a cooling fluid for power transformers

2.2.2.1. Magnetic properties

The full magnetization curve and the hysteresis loop of the transformer oil-based magnetic nanofluid (MNF/UTR 40), with a solid volume fraction of the dispersed magnetite particles of 1.67%, were measured at room temperature (25°C), using a vibrating sample magnetometer—VSM 880—ADE Technologies USA, in the magnetic field range of 0–950 kA/m.

The magnetization M measured at the maximum value of the applied magnetic field, approx. 900 kA/m, is considered to be the nominal magnetization of the investigated sample. Also, the absence of hysteresis loop area indicates a specific behavior of soft magnetic material (**Figure 6**) with the magnetic characteristics shown in **Table 2**.

In **Table 2**, M_r represents the remnant magnetization and H_c is the coercive magnetic field; ρ_{24^oC} is the density of the magnetic fluid at 24°C and $\varphi_{Fe_3O_4}$ is the solid volume fraction of the dispersed magnetite.

According to Shliomis [32], the magnetic behavior of a diluted magnetic nanofluid $(\varphi_{Fe_3O_4} < 5)$ under the action of an external magnetic field is well described by the single-particle model,

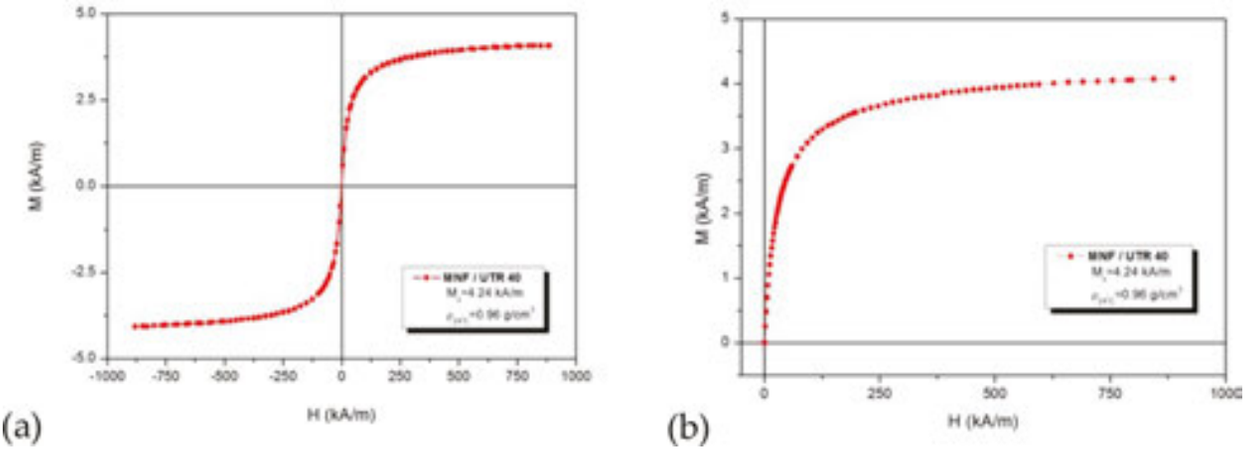

Figure 6. Hysteresis loop and full magnetization curve of the transformer oil-based magnetic fluid sample shows specific behavior of soft magnetic materials: (a) hysteresis loop for UTR 40-based MNF sample and (b) full magnetization curve for UTR 40-based MNF sample.

Sample	M (Gs)	M (kA/m)	M_r (kA/m)	H_c (kA/m)	ρ_{24^oC} (g/cm^3)	$\varphi_{Fe_3O_4}$ (%)
MNF/UTR 40	50	3.98	–	–	0.96	1.67

Table 2. Physical properties of MNF/UTR 40 sample.

which states that the energy of dipolar interactions is lower than the thermal energy. In this case, the equilibrium static magnetization is a superposition of Langevin functions,

$$M = \varphi_m M_d \left(\coth\xi - \frac{1}{\xi} \right) = \varphi_m M_d L(\xi), \tag{2}$$

with

$$\xi = \frac{\pi \mu_0 M_d D_m^3 H}{6 k_B T}, \tag{3}$$

representing the Langevin parameter. Herein $M_d = 480$ kA/m is the monodomenial magnetization of magnetite, $\mu_0 = 4\pi \times 10^{-7}$ H/m is the magnetic permeability of vacuum, D_m is the magnetic diameter of the dispersed magnetite particles, H is the applied magnetic field, $k_B = 1.38 \times 10^{-23}$ J/K is the Boltzmann constant and T is the absolute temperature.

In low magnetic fields (< 1 mT), with $\xi \to 0$, the Langevin function becomes $L(\xi) \to \frac{\xi}{3}$, that is a linear variation in sample magnetization with the applied field. Knowing that the initial magnetic susceptibility is $\chi_{iL} = M/H$, one can obtain:

$$\chi_{iL} = \frac{\pi \mu_0 \varphi_m M_d^2 D_m^3}{18 k_B T} \tag{4}$$

On the other hand, in the region of intense magnetic fields ($\xi >> 1$), the Langevin function is given by $L(\xi) \to 1 - \frac{1}{\xi}$ and static magnetization of the magnetic nanofluid is approximated by the following relationship [33],

$$M \cong \varphi_m M_d \left(1 - \frac{6k_B T}{\pi \mu_0 M_d D_m^3 H}\right), \tag{5}$$

where $\varphi_m = M_s/M_d$ is the magnetic volume fraction, with M_s representing the saturation magnetization of the magnetic nanofluid sample. The above relationship shows that the magnetization reaches saturation for very high values of the magnetic field $(H \to \infty)$.

In fact, in real ferrofluids, the dimensional polydispersity of the magnetic particles is a characteristic that cannot be neglected and, in the absence of inter-particle interactions, an accurate expression of magnetization is obtained [34],

$$M = M_s \int_0^\infty L(\xi) f(x) dx, \tag{6}$$

where $f(x)$ is the log-normal distribution function (**Figure 7**)

$$f(x) = \frac{1}{xS\sqrt{2\pi}} \exp\left(-\frac{\ln^2 \frac{x}{D_0}}{2S^2}\right), \tag{7}$$

with x is the magnetic diameter of the magnetite particles; $f(x)dx$ representing the probability that the magnetic diameter of the magnetic particles to be in the range of $(x;\ x + dx)$; D_0 is the dimensional distribution parameter, defined by the relationship $\ln(D_0) = \langle \ln(x) \rangle$; S is also a dimensional distribution parameter, representing the deviation of $\ln(x)$ value from $\ln(D_0)$ [35].

Another important aspect regarding the magnetization evaluation that should be considered is the dependence of the dispersed nanoparticles magnetic moments with their magnetic diameters [36, 37]. Here, $M_s(x) = nm(x)$ and the ferrofluid magnetization become

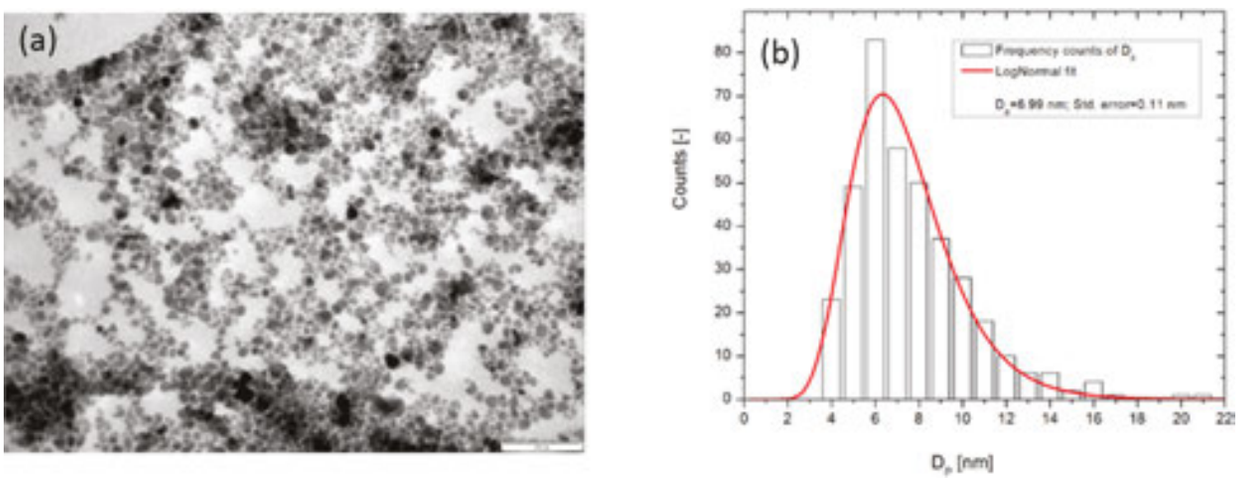

Figure 7. (a) TEM image of mono-layer covered magnetite nanoparticles with oleic acid and stably dispersed in hexane; (b) dimensional distribution of the magnetic particles physical diameters is well approximated by the log-normal distribution function.

$$M = n\int_0^\infty m(x)L(\xi)f(x)dx, \tag{8}$$

with n representing the density of the dispersed magnetite particles in magnetic fluid and m is the dipolar magnetic moment.

The linear dependence of the initial magnetic susceptibility versus magnetic particle concentration in low fields, rel. (4), and the asymptotic variation in magnetization in intense magnetic fields, rel. (5), form the basic instruments of magnetogranulometric analysis, in order to determine the mean magnetic diameter of the dispersed magnetic particles,

$$\langle D_m \rangle = D_0 \exp\left(\frac{S^2}{2}\right), \tag{9}$$

and standard deviation

$$\sigma = \sqrt{\langle D_m^2 \rangle - \langle D_m \rangle^2},$$

$$\sigma = D_0 \exp\left(\frac{S^2}{2}\right)[\exp S^2 - 1]^{1/2}, \tag{10}$$

where the dimensional distribution parameters are evaluated first,

$$S = \frac{1}{3}\sqrt{\ln\frac{3\chi_{iL}H_0}{M_s}}, \tag{11}$$

$$D_0^3 = \frac{6k_BT}{\pi\mu_0 M_d H_0}\sqrt{\frac{M_s}{3\chi_{iL}H_0}}, \tag{12}$$

and

$$n = \frac{\mu_0 M_s H_0}{k_B T}, \tag{13}$$

The expression of the dimensional distribution parameters was obtained from rel. (8), considering the above presented limit cases and evaluating the initial magnetic susceptibility and saturation magnetization, respectively.

In the linear region of small magnetic fields ($H < 1$ kA/m) from static magnetization curve, measured for the MNF/UTR 40 sample, the initial magnetic susceptibility has been evaluated. M_s and H_0 magnetic field were determined in the quasi-saturation region ($H > 700$ kA/m), where the contribution to the ferrofluid magnetization is given by the magnetic particle interactions with the applied magnetic field, inter-particle interactions being neglected. As a result, in the saturation region can be considered that the magnetic nanofluid magnetization varies linearly with 1/H according to Langevin's law, even for concentrated samples. In

Figure 8, which represents the final part (quasi-saturation) of the magnetization curve in $M = f(1/H)$ representation, M_s is obtained as the intersection with the ordinate axis. Also, the ratio of the magnetization curve slope and the corresponding absolute value of M_s is the value of H_0 field, where R^2 represents the measure of accuracy of the fit in linear regression (**Table 3**).

Magnetogranulometric analysis of the MNF/UTR 40 sample has revealed a mean magnetic diameter of the magnetite particles of $\langle D_m \rangle = 6.46$ nm and a standard deviation of $\sigma = 2.18$ nm. The log-normal distribution parameters (rel. (11)–(13)), evaluated directly from the magnetization curve, were obtained through non-linear regression, using rel. (8). Considering the thickness of non-magnetic layer at the surface of magnetic nanoparticles of $\delta_m = 0.83$ nm [33],

$$\langle D_p \rangle = \langle D_m \rangle + 2 \cdot \delta_m, \tag{14}$$

a value of 8.12 nm was determined for the mean physical diameter. Furthermore, a thickness of 1.9 nm of the oleic acid monolayer cover of magnetite particles δ_s [38] leads to a hydrodynamic diameter of the particles of $\langle D_h \rangle = 11.92$ nm,

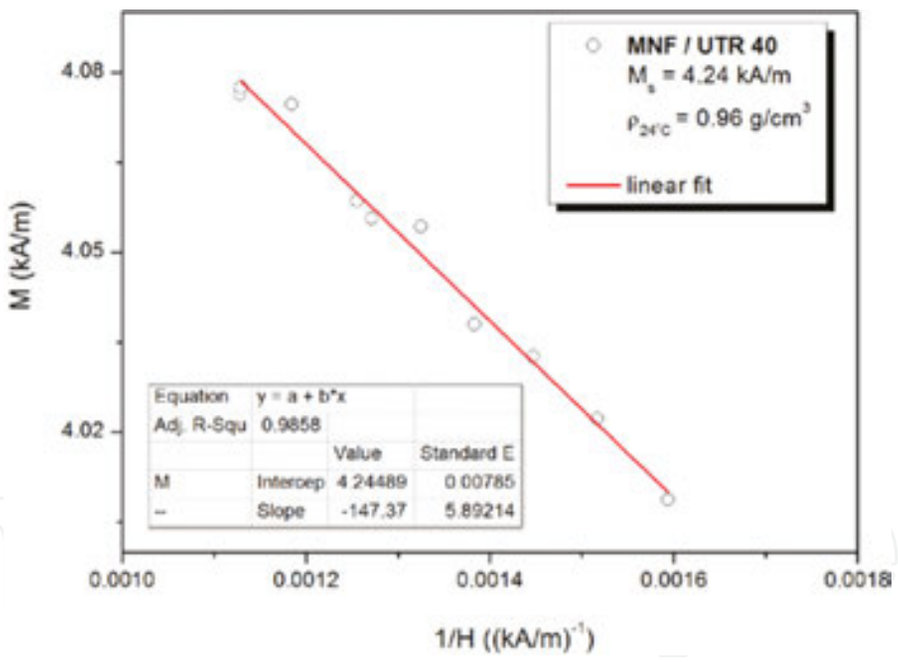

Figure 8. Obtaining M_s and H_0 field in the quasi-saturation region of the magnetization curve, in $M = f(1/H)$ representation, where the ferrofluid magnetization varies linearly with $1/H$, according to Langevin's law.

Sample	χ_{iL} (-)	R^2 (χ_{iL}) (-)	M_s (kA/m)	M_s (Gs)	H_0 (kA/m)	R^2 (M_s) (-)
MNF/UTR 40	0.11	0.99467	4.24	53.23	34.72	0.98580

Table 3. Initial magnetic susceptibility and saturation magnetization of the transformer oil-based magnetic fluid sample.

$$\langle D_h \rangle = \langle D_p \rangle + 2 \cdot \delta_s \tag{15}$$

Main results obtained through magnetogranulometric analysis of the MNF/UTR 40 sample are summarized in **Table 4**.

2.2.2.2. Rheological properties

Rheological investigations, carried out with an Anton Paar Physica MCR 300 rheometer using a double-gap concentric cylinder geometry, consisted of measuring the dynamic viscosity curves of the samples in the absence of the magnetic field. The shear rate, $\dot{\gamma}$, varied from 1 s^{-1} to 1000 s^{-1}, at different values of working temperature t = (20; 40; 60; 80)°C. The viscosity curves (**Figure 9**) measured for both the transformer oil-based magnetic nanofluid (MNF/UTR 40) and the carrier liquid-transformer oil (UTR 40) showed that adding a small volume fraction of magnetic particles in the carrier ($\phi_{Fe_3O_4} \cong 1.67\ \%$) leads to a very mild increase in the dynamic viscosity and the Newtonian behavior of the samples is preserved throughout the investigated temperature range.

This behavior indicates the absence of the magnetic particle interactions, that is, a very good stability of the sample, mainly due to the efficient steric stabilization. An Arrhenius-type relationship describes the sample viscosity behavior with temperature,

Sample	D_0 (nm)	S (-)	n (× 10^{22} partic./m^3)	$\langle D_m \rangle$ (nm)	σ (nm)	$\langle D_p \rangle$ (nm)	$\langle D_h \rangle$ (nm)
MNF/UTR 40	6.12	0.33	4.50	6.46	2.18	8.12	11.92

Table 4. Main properties of MNF/UTR 40 sample obtained through magnetogranulometric analysis, including the log-normal distribution parameters values.

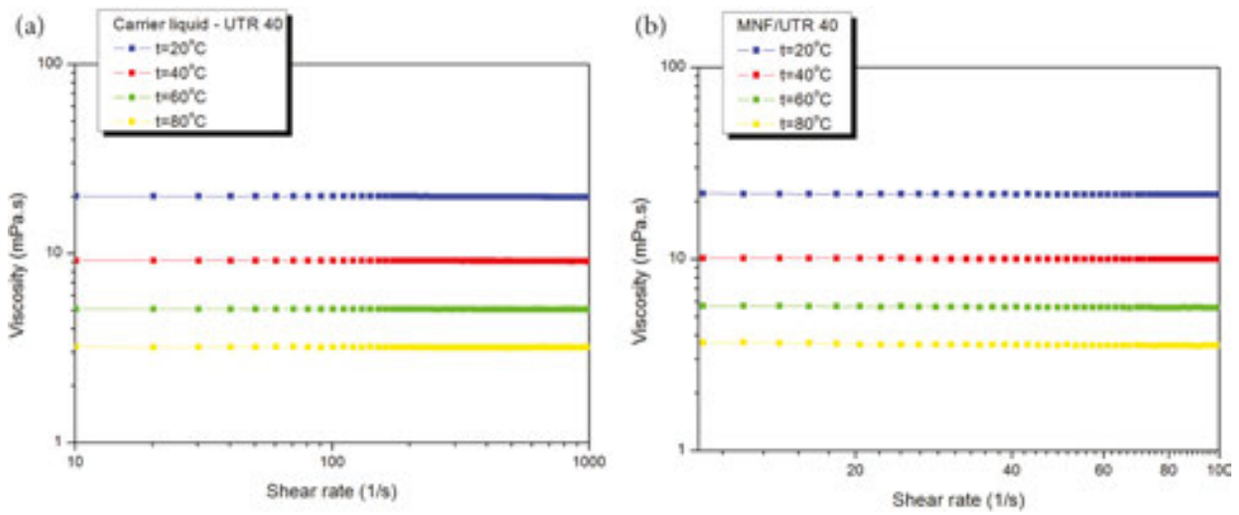

Figure 9. Viscosity curves showed that the Newtonian behavior of the carrier (UTR 40) (a) is preserved throughout the temperature range, also for the magnetic nanofluid (MNF/UTR 40), (b) that contains a small amount of the dispersed magnetic particles, indicating an efficient steric stabilization.

$$\eta = \eta_{\text{ref}} \exp\left[-\frac{\text{Ea}}{\text{R}}\left(\frac{1}{\text{T}}-\frac{1}{\text{T}_{\text{ref}}}\right)\right], \tag{16}$$

where $\text{T}_{\text{ref}} = 20^{\text{o}}\text{C}$ is considered the reference temperature; $\eta_{\text{ref}}(\text{Pa}\cdot\text{s})$ is the dynamic viscosity corresponding to the reference absolute temperature; $E_{\text{a}}\ (\text{J}\cdot\text{mol}^{-1})$ means the activation energy and $\text{R} = 8.31447\ \text{J}\cdot\text{mol}^{-1}\text{K}^{-1}$ is the ideal gas constant.

Considering a shear rate of 100 s^{-1}, rel. (16) was used to fit the dependence $\eta = \eta(\text{T})$, with activation energy as fit parameter (**Figure 10**).

In **Table 5**, it can be observed that the value of the viscous flow activation energy does not change after dispersing a small amount of surfacted magnetite particles in the carrier liquid. It can be concluded that the adding of small volume fractions of surfacted magnetite particles in a carrier liquid($\varphi_{\text{Fe}_3\text{O}_4} < 5$), as transformer oil, has no significant influence on the rheological properties of the samples.

2.2.2.3. Thermal properties

The addition of metallic nanoparticles (magnetic or non-magnetic) or non-metallic (e.g., diamond nanoparticles) in transformer oils in order to improve their cooling performances is a solution that was demonstrated by several patents and associated research works (e.g. [39–45]). This paragraph analyzes the thermal properties of the magnetic nanofluid, which was tested for use as cooling and insulating medium in power transformers.

Determination of the effective thermal properties that characterize the cooling fluids in our study as well as their modeling using analytical formulae is representing a main problem of the topic in discussion. Irrespective of the considered approach, either theoretical or experimental, a representative element of the studied medium has to be chosen. It has to be

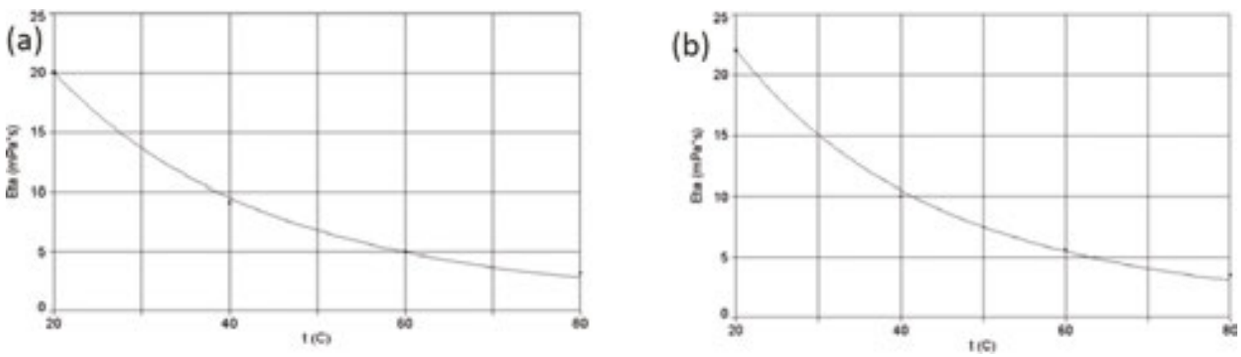

Figure 10. Arrhenius type dependence of the samples dynamic viscosity with temperature: (a) carrier liquid UTR 40 and (b) transformer oil-based magnetic nanofluid MNF/UTR 40.

Sample	$\phi_{\text{Fe}_3\text{O}_4}$ (%)	$E_{\text{a}}(\text{J}\cdot\text{mol}^{-1})$
MNF/UTR 40	1.67	28.27×10^3
UTR 40	–	28.38×10^3

Table 5. Viscous flow activation energy of the carrier liquid (UTR 40) and the magnetic nanofluid (MNF/UTR 40).

underlined that the determination of the properties of heterogeneous materials has to be made by complying with the request of representativeness of the studied volume, that is, the considered volume of the heterogeneous material must be sufficiently large in order to be statistically representative irrespective of the type of the carried out experiment [46, 47].

The main properties that are influencing the thermal behaviour of a material are the heat capacity, thermal conductivity, density, thermal expansion coefficient and thermal diffusivity (a property that depends on the first three). Various experimental studies determined that the effective properties of nanofluids (magnetic or non-magnetic) are dependent on the following characteristics of their components [25, 48–50]: the thermo-physical properties of the carrier fluid, nanoparticles and surfactant; nanoparticles volume fraction, size distribution, mean diameter and shape; temperature; magnetic field (in the case of magnetic nanoparticles).

A review of the reference literature regarding the main properties of the transformer oil-based fluids and their dependence with the temperature outlined the followings: specific heat is increasing as linear function with temperature; thermal conductivity is decreasing as a quasi-linear function with temperature especially for transformer oils; dynamic viscosity is decreasing with the increasing temperature; the dielectric constant has relatively low values and decreases with the increasing temperature [51–53].

2.2.2.3.1. Thermal conductivity

The thermal conductivity of magnetic nanofluids can be described as a function of several parameters, among the most important are the thermal conductivities of the carrier liquid and magnetic nanoparticles and their dependence on temperature and pressure, the volume fraction, the shape and the size distribution of the nanoparticles. The interfacial thermal resistance between the nanoparticles and the surrounding liquid is also considered. It has been proved numerically and experimentally that an applied magnetic field can affect the thermal conductivity of a magnetic nanofluid due to the consequent ordering of magnetic dipoles of the nanoparticles along the field lines [25, 54].

There are many Maxwell-type models developed for the thermal conductivity of mixtures (also named effective thermal conductivity—ETC), either solid matrix—solid filler or liquid carrier and dispersed nanoparticles that are based on the Maxwell model, which is recommended for low volume fraction of the filler/nanoparticles and considers that the nanoparticles are identical, spherical and non-interacting. The Holotescu-Stoian model, developed initially for the solid matrix—solid filler mixture and presented in Refs. [55, 56], introduced for the first time the filler particle size distribution in the Maxwell model. The expression for the effective thermal conductivity of the Holotescu-Stoian model, rel. (17), in the case of a magnetic nanofluid is [57],

$$k_e = k_f \frac{k_p + 2\,k_f + 2\ \varphi_e\,(k_p - k_f)}{k_p + 2\,k_f - \ \varphi_e\,(k_p - k_f)}, \tag{17}$$

where k_e is the effective thermal conductivity of the magnetic nanofluid, k_p is the thermal conductivity of the magnetic nanoparticles, k_f is the thermal conductivity of the carrier fluid, φ_e is the equivalent volume fraction, defined by

$$\varphi_e = \varphi_{Fe_3O_4} \frac{\langle (D_m + \delta)^3 \rangle^2}{\langle (D_m + \delta)^2 \rangle^3}, \tag{18}$$

with $\varphi_{Fe_3O_4}$ is the solid nanoparticles volume fraction (magnetite in this case),D_m is the magnetic diameter, $\delta = 2\delta_m$ is the double thickness of the non-magnetic layer, and

$$\langle u \rangle = \int_0^\infty uf(x)dx \tag{19}$$

with u being a magnetic diameter dependent function and f(x) is the log-normal distribution function.

The relationship between physical (geometrical) diameter D_p, magnetic diameter D_m and δ is given by

$$D_p = D_m + \delta. \tag{20}$$

This model, confirmed by the experimental data [57], was applied to determine the thermal conductivity of the analyzed magnetic nanofluid sample. The results (at room temperature) are given in **Table 6**, and we observe that the addition of magnetite nanoparticles alone is increasing the thermal conductivity of the magnetic nanofluid. The transformer oil thermal conductivity is decreasing with the increasing temperature, thus the cooling performance can be diminished at normal operating conditions in power transformers (and other electrical equipments). We can conclude that the addition of the magnetite nanoparticles can counteract this disadvantage. Moreover, during the operation of a power transformer, for instance, the magnetic field is acting on the magnetic nanofluid, influencing its physical properties, and generating the magneto-convection that can enhance the heat transfer, as shown in the next section.

2.2.2.3.2. Specific heat

The specific heat of the magnetic nanofluid, at constant pressure, was determined using the following mixture formula [58]

$$\rho_{MNF}(T) \cdot c_{p,MNF}(T) = (1-\varphi) \cdot \rho_{UTR}(T) \cdot c_{p,UTR}(T) + \varphi_m \cdot \rho_{NP}(T) \cdot c_{p,NP}(T), \tag{21}$$

where the transformer oil specific heat was determined by using

$$c_{p,UTR}(T) = 5.025 \cdot T + 1789.50 \tag{22}$$

and the specific heat of the magnetite by using [59],

Property/sample	UTR	NP	MNF_UTR	$\Delta X/X_{UTR}$
k_e (W/m K)	0.127	1.39	0.135	+6.29%
c_p (J/kg K)	1910.1	0.892	1867.8	−2.2%
β (1/K)	7.15×10^{-4}	1.2×10^{-4}	6.44×10^{-4}	−9.94%

Table 6. Thermal expansion coefficients.

$$c_{p,\,NP}(T) = 0.6334 + 0.871 \cdot 10^{-3}T, \tag{23}$$

where T (K) is the absolute temperature of the solid and ρ is the mass density of the material.

The numerical results obtained for the magnetic nanofluid specific heat indicate a slightly decrease compared to that of the carrier liquid. In what it concerns the effect of an applied magnetic field on the specific heat capacity of a magnetic nanofluid, for a certain range of temperature, the reference literature indicates the influence of the nanoparticles volume fraction and nanofluid composition (carrier liquid and nanoparticles). Also, the magnitude and the applied field orientation relative to the gravitational field (as the experiments were conducted in gravitational field) should be considered. Korolev et al. [60] analyzed the influence of an applied magnetic field (oriented perpendicularly on gravity) on a transformer oil-based magnetic nanofluid with magnetite nanoparticles, having a solid volume fraction of 7.4%, in the temperature range from 15 to 80°C. The experiment showed that, for a certain temperature, the specific heat capacity has a maximum in the investigated range of the applied magnetic field, which, according to the authors, indicates the presence of a magneto-caloric effect.

2.2.2.3.3. Thermal expansion coefficient

Similarly, to determine the thermal expansion coefficient of the magnetic nanofluid, a corresponding mixing formula was used [61],

$$\beta_{MNF} = \beta_{UTR}\left[\frac{1}{1+\frac{(1-\varphi_{Fe_3O_4})\rho_{UTR}}{\varphi_{Fe_3O_4}\rho_{NP}}}\frac{\beta_{NP}}{\beta_{UTR}} + \frac{1}{1+\frac{\varphi_{Fe_3O_4}}{1-\varphi_{Fe_3O_4}}\cdot\frac{\rho_{NP}}{\rho_{UTR}}}\right], \tag{24}$$

where β_{MNF} [1/K] is the thermal expansion coefficient of MNF, β_{UTR} is the thermal expansion coefficient of the transformer oil [62], β_{NP} is the thermal expansion coefficient of the magnetite nanoparticles [63], $\rho_{UTR} = 0.867\ g/cm^3$ (at 20°C) and $\rho_{MNF} = 0.96\ g/cm^3$ (at 24°C) are the measured densities of the transformer oil and the magnetic nanofluid, respectively.

The results of the calculations, summarized in **Table 6**, give the thermal properties at room temperature. We observe that the analyzed thermal properties have a diverging behavior. While the thermal expansion coefficient and specific heat are decreasing, the thermal conductivity is increasing. The last column is indicating the relative variation compared to the corresponding property of the carrier liquid (transformer oil).

2.2.2.3.4. Evaluation of the heat transfer potential of the magnetic nanofluid

To determine the potential performance of the magnetic nanofluid for heat transfer, we considered the figure-of-merit (FOM), as defined for natural convection [64],

$$FOM_{NC} = \left[\beta\,\rho^2\,c_p\,k^{\frac{1}{n-1}}/\eta\right]^n, \tag{25}$$

where $n = 0.25$ for laminar flow and $n = 0.33$ for turbulent flow.

Property/sample	UTR	MNF_UTR	$\Delta X/X_{UTR}$
FOM, n = 0.25	18.61	19.57	+5.15%
FOM, n = 0.33	91.85	96.25	+4.8%

Table 7. FOM results, obtained for the carrier liquid and for the magnetic nanofluid.

Property/sample	UTR	NP	MNF_UTR	$\Delta\varepsilon / \varepsilon_{UTR}$
ε (F/m)	$2.2 \times \varepsilon_0$	$81 \times \varepsilon_0$	$2.26 \times \varepsilon_0$	2.85%

Table 8. Effective electric permittivity of the Fe_3O_4 transformer oil-based magnetic nanofluid.

The results obtained for the FOM of the carrier liquid and the magnetic nanofluid, using the properties determined above, are presented in **Table 7**. The comparison of the relative increase of FOM indicates that the addition of nanoparticles is advantageous for both laminar and turbulent flow.

2.2.2.4. Electric permittivity

As underlined above, the use of a magnetic nanofluid in electrical engineering applications imposes restrictions regarding its insulating properties. Transformer oils are known to be electrical insulators so they are an appropriate carrier liquid for a magnetic nanofluid used in such applications. If the magnetic nanoparticles volume fraction is kept in certain limits, the magnetic nanofluid preserves its insulating properties within the required limits, too [49, 50].

We estimated the effective electric permittivity of the magnetic nanofluid ε_{MNF}, using the Maxwell-Garnett equation for mixtures:

$$\varepsilon_{MNF} = \varepsilon_{UTR} + 3\varphi_{Fe_3O_4}\varepsilon_{UTR}\frac{\varepsilon_{NP}-\varepsilon_{UTR}}{\varepsilon_{NP}+2\varepsilon_{UTR}-\varphi_{Fe_3O_4}(\varepsilon_{NP}-\varepsilon_{UTR})}, \tag{26}$$

with ε_{UTR} is the electric permittivity of the transformer oil and ε_{NP} is the electric permittivity of the magnetite nanoparticles, $\varphi_{Fe_3O_4}$ being the volume fraction of the magnetite nanoparticles.

The results are presented in **Table 8**, along with the relative difference between the values corresponding to the transformer oil and magnetic nanofluid, ε_0 being the free space permittivity, approximate equal to 8.85×10^{-12} F/m.

We observed that for the current volume fraction of magnetic nanoparticles, the insulating properties of the magnetic nanofluid remain very close to those of the carrier liquid (UTR 40). In what concerns the effect of working temperatures in the power transformer, experimental studies showed that electrical permittivity decreases with increasing temperature in the case of transformer oils [51].

3. Heat transfer and electromagnetic field by numerical simulation for the electrical transformer cooled by a specific nanofluid

A colloidal Fe_3O_4 specific nanofluid dispersed in oil transformer UTR 40, named MNF/UTR 40, is utilized in a number of technologically relevant applications where external magnetic fields are used to adjust their flow. A mathematical model and numerical simulation results are useful for investigating the heat transfer properties of the magnetic nanofluid. Based on this study, it was built and tested the experimental model: low power, medium voltage, single-phased transformer type TMOf-24-5" (**Figure 18**) and low power, medium voltage, single-phased transformer type TMOf2-36kV-40 kVA (**Figure 19**). First of all, it was used for the transformer the transformer oil UTR 40 as cooling and insulating liquid. After that, this oil was drained and the experimental model was filled with magnetic nanofluid based on transformer oil MNF/UTR 40. The MNF/UTR 40 specific nanofluid has been shown to provide both thermal and dielectric benefits to transformers, and can be utilized to improve cooling by enhancing fluid circulation within transformer windings, to increase transformer capacity to withstand lightning impulses, while also minimizing the effect of moisture on typical insulating fluids. Magnetic nanofluid flow may be influenced by external magnetic fields, and the retention force of a magnetic nanofluid can be adjusted by changing either the magnetization of the fluid or the magnetic field in the region. Opposite to usual magnetic fluids, the magnetizable nanofluids destined to heat transfer should have a low concentration of magnetic nanoparticles in order to make them competitive with the non-magnetic fluids.

3.1. Mathematical model

Several simplifying assumptions aimed and keeping the physical system within approachable software and hardware limits are requested and 2D models are best candidates, providing numerical simulation relevant results, of satisfactory accuracy. Following this path, we consider a 2D, Cartesian cross-sectional model, as shown in **Figure 11**.

The heat transfer and transport processes under the influence of the magnetic field for two prototypes electric transformer: low power mono-phased transformer (24 kVA), at medium voltage (20/√3//0,4/√3kV), TMOf-24-5 and low power mono-phased transformer (40 kVA), at medium voltage (30/√3//0,4/√3kV), prototype TMOf 2-36kV-40 kVA, are described by the following set of coupled partial differential equations [44]:

- electromagnetic field—quasi-steady, harmonic diffusion,

$$(j\omega\sigma - \omega^2\varepsilon_0\varepsilon_r)\mathbf{A} + \nabla\times(\mu_0^{-1}\mu_r^{-1}\nabla\times\mathbf{A}) - \sigma u\times(\nabla\times\mathbf{A}) = J^e, \tag{27}$$

- momentum balance (Navier-Stokes),

$$\rho\left[\frac{\partial\mathbf{u}}{\partial t} + (\mathbf{u}\cdot\nabla)\mathbf{u}\right] = -\nabla p + \underbrace{\mu_0(\mathbf{M}\cdot\nabla)\mathbf{H}}_{f_{mg}} + \mu_f\nabla^2\mathbf{u} + \mathbf{f}_T, \tag{28}$$

- mass conservation (incompressible flow),

$$\nabla \mathbf{u} = 0, \tag{29}$$

- heat transfer (energy equation),

$$\rho c_p \left[\frac{\partial T}{\partial t} + (\mathbf{u} \cdot \nabla)T\right] = k\nabla^2 T + \mathbf{E} \cdot \mathbf{J}_{\varphi}^{e}. \tag{30}$$

Here: u is the velocity; p is the pressure; **T** is the absolute temperature; **A** is the magnetic vector field; **M** is the magnetization (in the magnetic nanofluid); **H** is the magnetic field strength; E is the electric field strength; $\mathbf{J}_{\varphi}^{e}$ is the angular component of the (external) current density (in the coil); $\mathbf{f}_T$ is the buoyancy body force term; $\mathbf{f}_{mg}$ is the magnetic body force term; σ is the electrical conductivity; k is the thermal conductivity; μ_0 is the magnetic permeability of vacuum ($\mu_{air} = \mu_{r\ air} \cdot \mu_0 \cong \mu_0$; $\mu_{r\ air} \cong 1$); μ_f is the kinematic viscosity; ρ is the mass density; c_p is the specific heat. Heat transfer occurs by conduction in the solid regions of the system and by convection and diffusion in the fluid region. The temperature variation in the fluid region is responsible for a gravitational flow (Boussinesq approximation), whose structure depends on the cell geometric aspect ratio and thermal conditions. All subdomains have linear physical

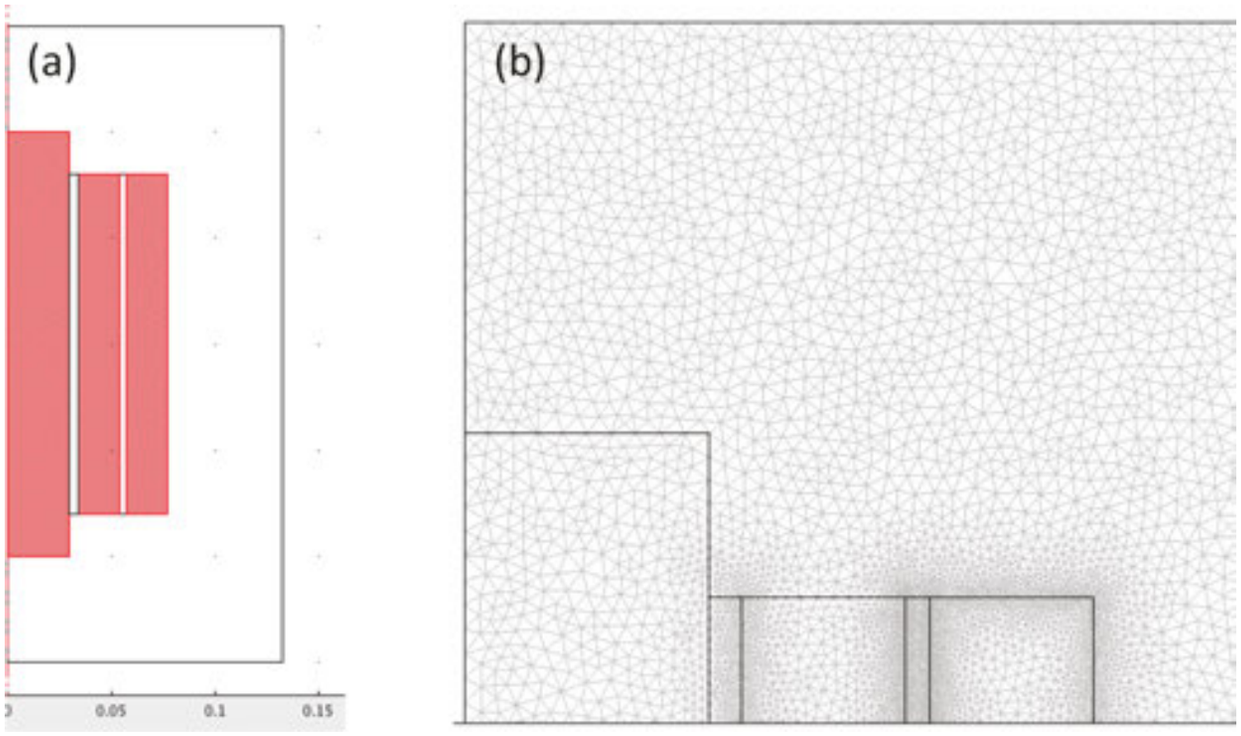

Figure 11. The 2D simplified model and the FEM mesh made of triangular elements: (a) computational domain and (b) detailed view—windings, iron core, case.

properties, except for the magnetic nanofluid (based on transformer oil), whose magnetization characteristic is nonlinear.

The magnetic field magnetizes the magnetic nanofluid, and the corresponding body force term adds to the gravitational, thermal flow of the magnetic nanofluid coolant. The flow structure is the result of the two competing forces: thermal force and magnetic force. In this study, we deal with a super-paramagnetic magnetic nanofluid where the influence of the coercive magnetic field intensity, H_c or the remnant induction, B_r is discarded. The constitutive law for the magnetic field of the magnetic fluid is then

$$\mathbf{B} = \mu_0(\mathbf{H} + \mathbf{M}). \tag{31}$$

The magnetic field produced by the electrical current in the coil magnetizes the fluid and is responsible for the magnetic body forces that influence the thermally induced flow. The magnetization of the magnetic fluid is approximated here by the analytic formula

$$M_{x,y} = a \cdot \arctan(b \cdot H_{x,y}), \tag{32}$$

with $a = 10^4 A/m$ and $b = 3 \times 10^{-5} m/A$ are empiric constants. The magnetic body forces are then obtained out of the magnetic energy, by taking its derivatives with respect to the coordinates

$$f_{mg} = \mu_0(\mathbf{M} \cdot \nabla)\mathbf{H}. \tag{33}$$

The strategy that we used in the numerical simulation consists of solving for the magnetic field first, and then using the active power thus obtained as heat source in the heat transfer and flow parts of the problem. The obtained solutions are steady state [65] for heat transfer and flow and quasi-steady (harmonic) for the electromagnetic field.

The main dimensions (windings, iron core, case sizes) are those of the single-phased transformer considered in our study. The amperturns of the windings correspond to the nominal working point, when the iron core exhibits lower levels of magnetization—the amperturns are compensated.

3.2. Simulation results for mono-phased transformer of low power and medium voltage type TMOf-24-5 compared to the mono-phased transformer of low power and medium voltage type TMOf2-36kV-40 kVA

Numerical simulation of the mono-phased transformer of low power and medium voltage type TMOf-24-5 evidenced that the convective heat transfer in the channels between the windings and between the windings and core (3–5 mm) is less important in the overall process, therefore it was discarded, and only conduction heat transfer was accounted for in these areas. **Figure 12** shows simulation results for a non-magnetic, regular cooling fluid—the temperature field (surface color map, **Figure 12a–d**), the thermal flow (streamlines and velocity vectors, **Figure 12a–c**), magnetic flux density (**Figure 12d**, surface color map, iso-lines of magnetic

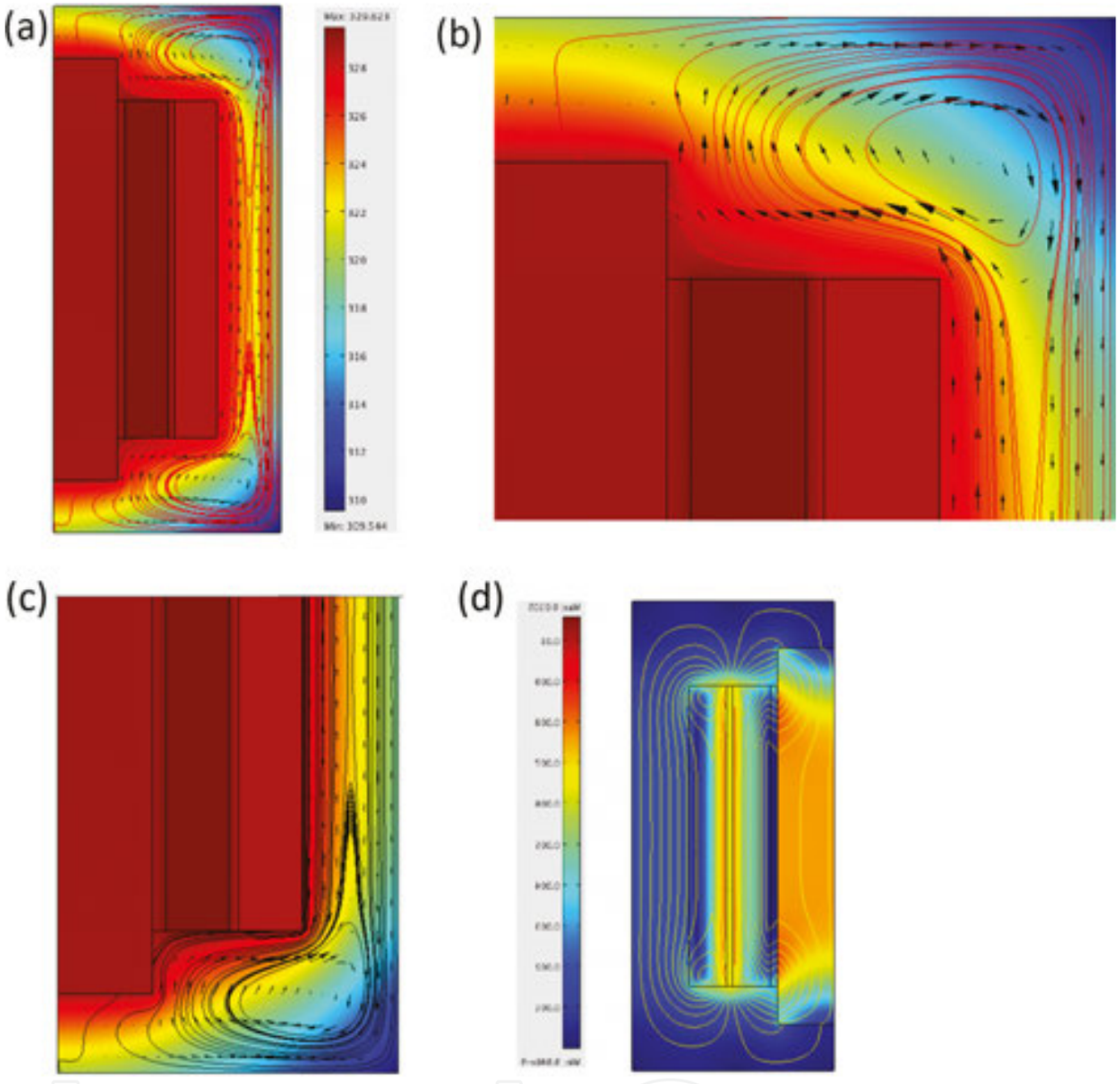

Figure 12. Magnetic field, temperature and flow fields for mono-phased transformer of low power and medium voltage, type TMOf-24-5, (a) Heat transfer and thermal flow—upper part, (b) detail—temperature, buoyancy flow, (c) heat transfer and thermal flow—bottom part and (d) magnetic field.

vector field). Apparently, the thermal flow exhibits two minor recirculation areas—in the upper and lower part of the windings, by the top and bottom covers—trapped within a larger recirculation cell that develops by the lateral wall. For the heat transfer part of the problem, we assumed a convection (Robin) type boundary condition (the ambient temperature was assumed to be $T_{amb} = 300$ K, with a heat transfer coefficient of $h = 2$ W/m^{2}K, that is, moderate natural convection.

The iron core, although less magnetized in this particular regime (compensated primary and secondary amperturns), plays a crucial role in the heat transfer problem.

http://dx.doi.org/10.5772/65556

When a colloidal Fe_3O_4 specific nanofluid MNF/UTR 40 is utilized as a coolant, magnetic body forces add to the thermal, gravitational body forces. **Figure 13** displays the magnetic field and forces (magnetic and thermal). Apparently, the magnetic forces contribute differently to the overall convection flow: in the upper part of the cell they add to the buoyancy forces, whereas in the lower part they are opposite. However not unexpected, Eq. rel. (33), another important finding is the effect that the en-parts of the windings and the iron core have: these are regions of high gradient magnetic field strength, and it is here that the body magnetization forces are significant. The orientation of the magnetic forces versus the thermal forces is an important factor in providing an optimal design. We observe that the thermal gravitationally driven forces and the magnetic forces act concurrently in this plane, their combined effect being greater at the left and right end regions. Similarly, the heat transfer direction is from the hotter regions (core and windings) to the case, but with enhanced convection and increased heat removal efficiency. Comparing the two cooling options, that is, specific nanofluid MNF/UTR 40 (**Figure 14b**) versus regular coolant UTR 40 (**Figure 14a**) apparently the MNF/UTR 40 may do better in cooling the transformer. This essentially means a lower hot spot temperature by approximately 10° in this model and a more uniform temperature distribution. These results suggest that the vertical design of the low-power mono-phased transformer (40 kVA), at medium voltage (30/√3//0,4/√3kV) prototype TMOf 2-36kV-40kVA (**Figure 15**) may be advisable [66, 67]. This prototype TMOf 2-36kV-40kVA realized in compliance with the constructive

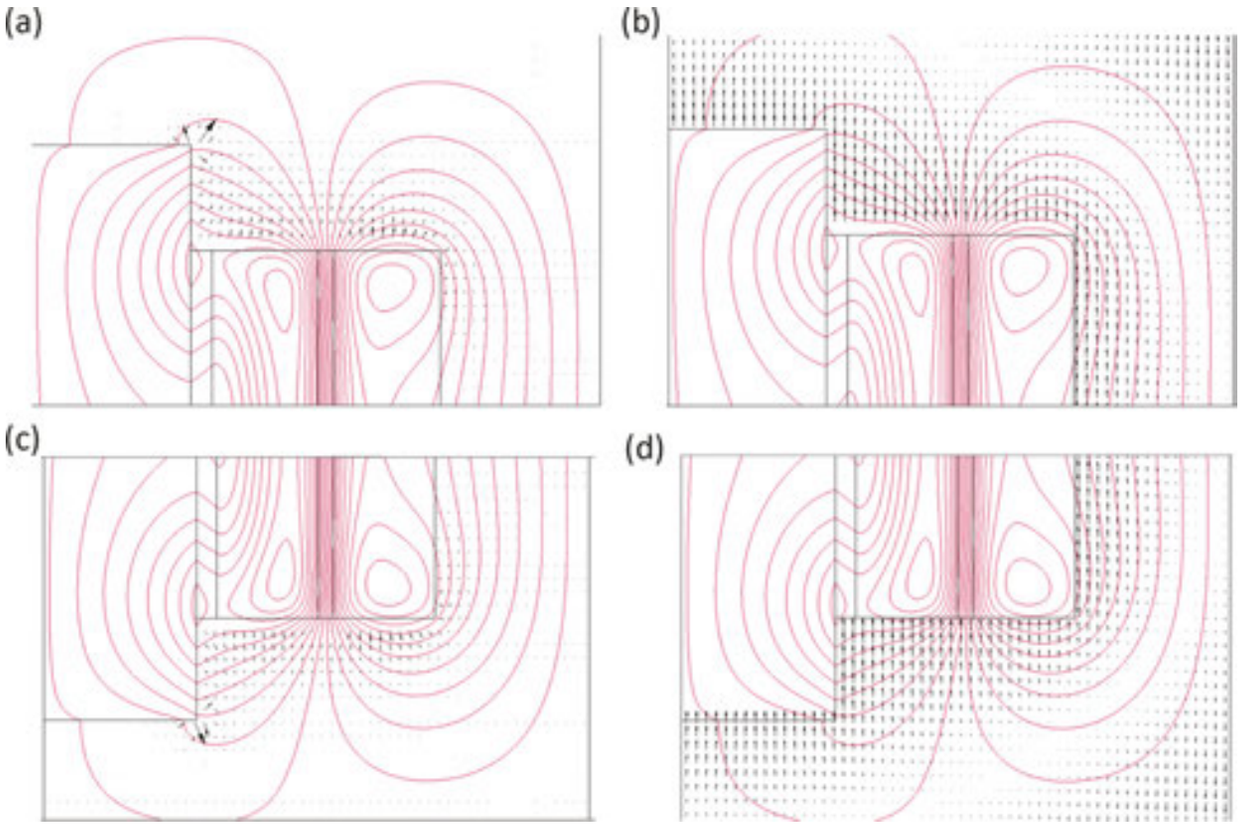

Figure 13. Magnetic field and body forces when the coolant is a magnetic nanofluid, MNF/UTR 40: (a) detail (top)—magnetic body forces, (b) detail (top)—buoyancy forces, (c) detail (bottom)—magnetic body forces, (d) detail (bottom)—buoyancy forces.

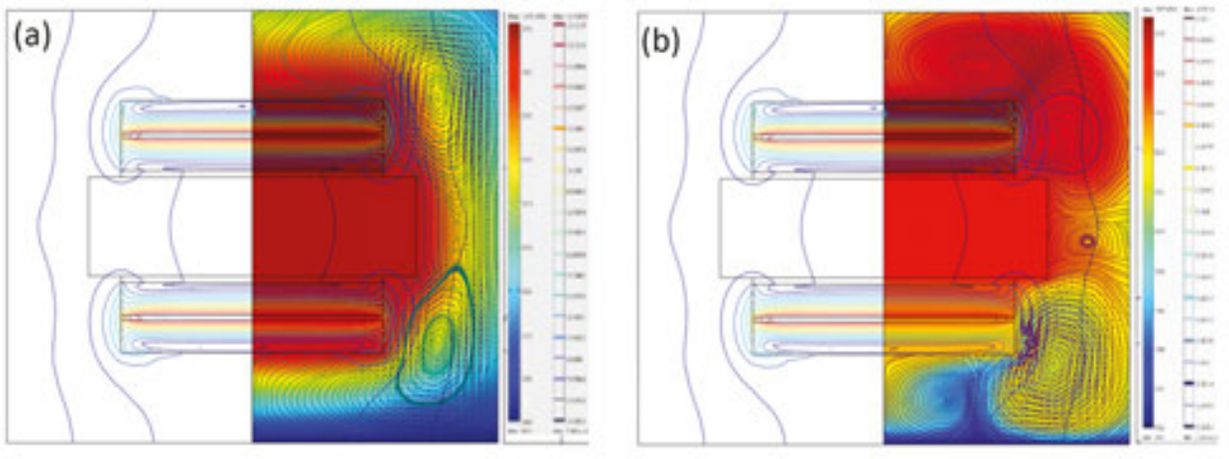

Figure 14. 2D, axial model - magnetic flux density field, temperature distribution, and flow field for the horizontal design TMOf-24-5 type transformer: (a) the coolant is regular UTR 40 transformer oil and (b) the coolant is a magnetic nanofluid, MNF/UTR 40.

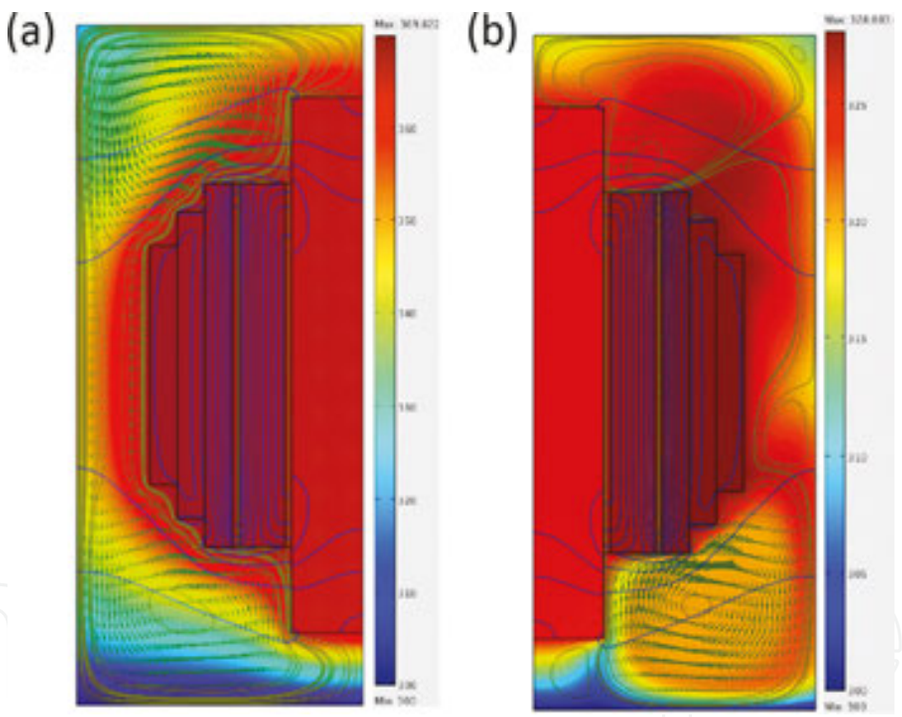

Figure 15. 2D, axial model - magnetic flux density field, temperature distribution, and flow field for the vertical design TMOf 2-36kV-40kVA type transformer: (a) the coolant is regular UTR 40 transformer oil and (b) the coolant is a magnetic nanofluid, MNF/UTR 40.

solutions with characteristics specific for the aimed purpose presents the following advantages: reduced weight and dimensions in comparison with the current power transformers that have the same rated voltage and rated power, following the intensification of the cooling effect in the presence of the specific nanofluid MNF/UTR 40 (**Figure 15b**). The number of convection zones is greater when the coolant is magnetic nanofluid MNF/UTR 40

http://dx.doi.org/10.5772/65556

(**Figure 15b**) as compared to the regular coolant, that is, the UTR 40 transformer oil (**Figure 15a**). Also, because of the execution form of the magnetic circuit and of the metallic construction (tank-bottom-lid), the construction of the power transformer in the aggregate is realized with a smaller consumption of the main materials: copper, magnetic steel sheet and the specific nanofluid MNF/UTR 40 are included.

4. Designing the electrical transformer cooled by nanofluid with colloidal magnetic Fe_3O_4 nanoparticles dispersed in UTR 40 transformer oil

The low-power mono-phased transformer (40 kVA), at medium voltage (30/√3//0,4/√3kV), prototype vertical design TMOf 2-36kV-40kVA type transformer has the active part (**Figures 16** and **17**), magnetic iron core with the high voltage (HV) and low voltage (LV) windings fixed in

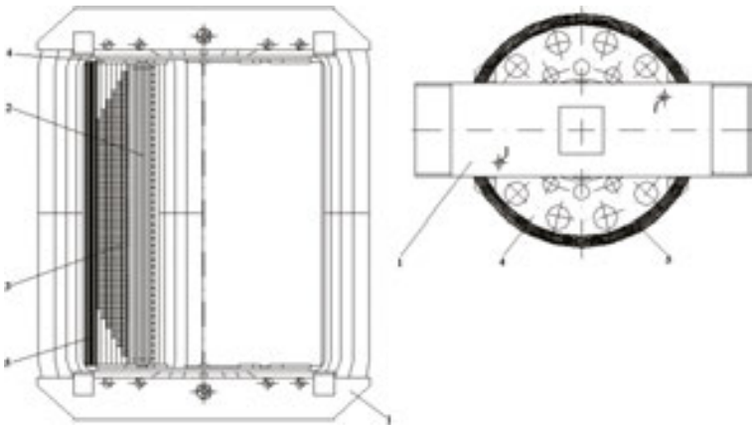

Figure 16. The aggregate active parts, core and windings [44].

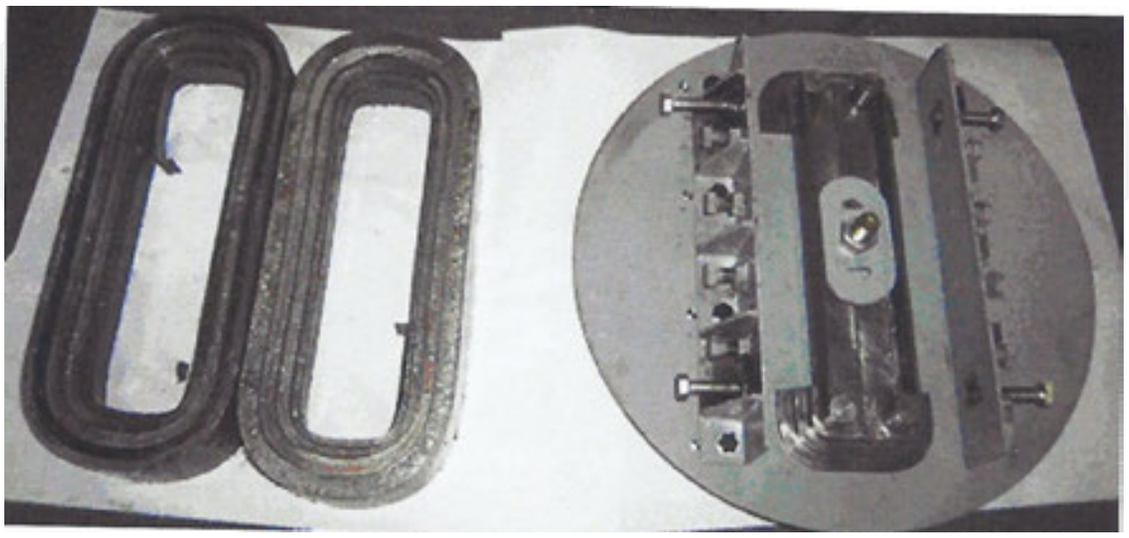

Figure 17. Magnetic cores and the core rolling device [44].

a finned metallic tank constituted from two parts air-proof assembled through a soldering that is soft and capable of elastic deformation for the taking-over of the variation with temperature of the cooling liquid volume (**Figure 19**). The magnetic circuit is coating type, constituted of two identical cores of rectangular shape (flat-core), back to back disposal (**Figure 17**). The aggregate active parts (**Figure 16**) are the magnetic core with the high voltage and low voltage windings, fixed on a metallic lid with their axes in a vertical position, the most convenient situation for the heat transfer enhancement by the nanoparticles in the presence of the electromagnetic field. With a view to performing comparative tests related to the use of magnetic nanofluid MNF/UTR 40 as cooling and insulating fluid transformers and regular UTR 40 transformer oil cooling, the mono-phased transformer of low power and medium voltage, the horizontal design TMOf-24-5 type transformer (**Figure 18**) and mono-phased transformer of low power and medium voltage the vertical design TMOf 2-36kV-40kVA type transformer (**Figure 19**) has been achieved [44]. The numerical simulation results show that the direction of the magnetizing force in comparison with the gravitational thermal force is an important

Figure 18. Mono-phased transformer of low power and medium voltage, the horizontal design TMOf-24-5 type transformer.

http://dx.doi.org/10.5772/65556

Figure 19. Mono-phased transformer of low power and medium voltage, the vertical design TMOf 2-36kV-40kVA type transformer [44].

element in assuring of an optimal heat transfer. Both numerical simulations as well as laboratory measurements [65–67] confirm the following aspects: about the usage of a magnetic nanofluid MNF/UTR 40 as cooling and insulating fluid for transformers, this provides for magnetization body forces that add to the thermal, gravitational forces. In the vertical layout of the transformer, these forces act concurrently with the thermal flow, and the overall effect is the enhancement of the heat transferred from the aggregate active parts (core and windings) to the ambient.

In both cases, first of all, the regular UTR 40 transformer oil as cooling and insulating fluid was used for the transformers. After that, this oil was drained and the transformers were filled with magnetic nanofluid MNF/UTR 40 as cooling and insulating fluid.

Figures 20 and **21** show the temperature on the surface of the ribbed tank when magnetic nanofluid MNF/UTR 40 is used for the vertical design TMOf 2-36kV-40kVA type transformer after 1 h of operation. Monitoring of the temperature was achieved with the thermographic camera, FLUKE Ti 20. The temperature does not exceed the value of 54°C. Magnetic nanofluid

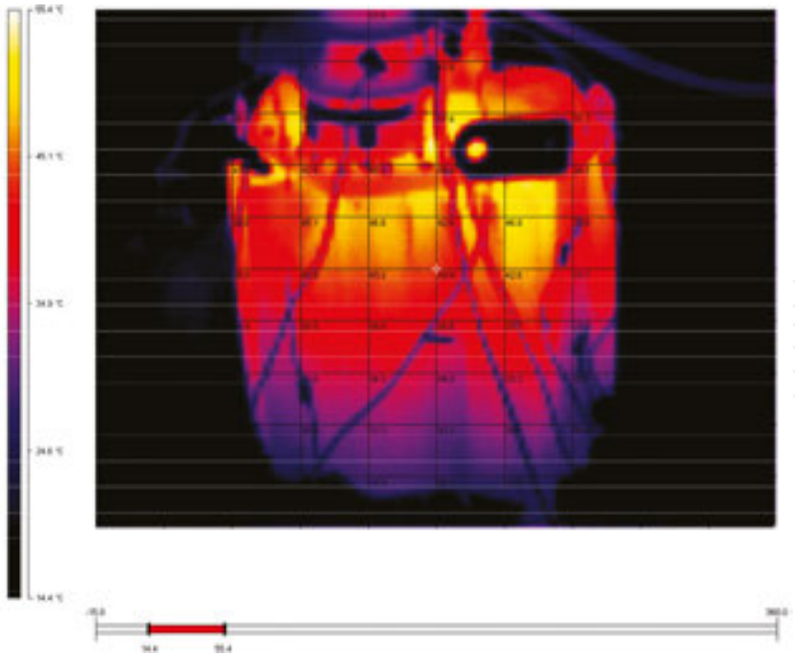

Figure 20. Temperature distribution by thermographic imaging-the tank- for mono-phased transformer of low power and medium voltage, type TMOf2-36kV-40 kVA, after 1 h of operation.

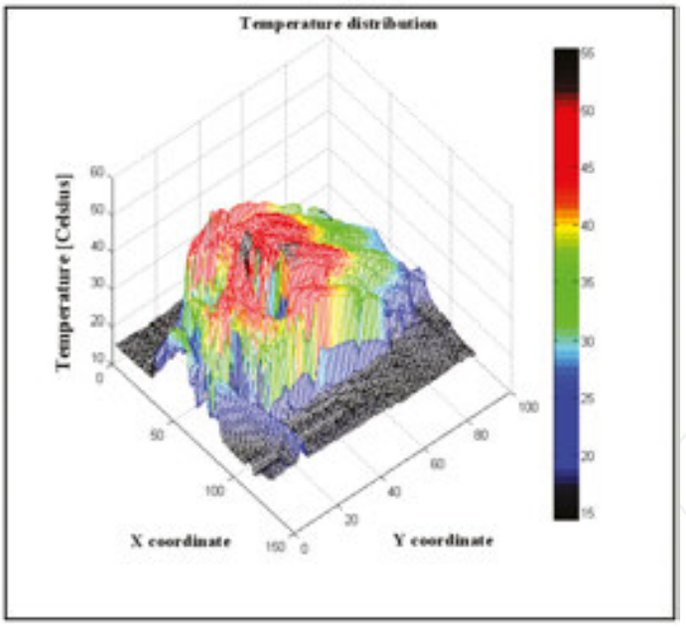

Figure 21. 3D characteristic of the temperature depending on the *X* and *Y* coordinates, associated with the thermographic image in **Figure 20**.

MNF/UTR 40 provides also the increase of the transformer's capacity to sustain over-voltages and withstand better to degradation in time due to humidity, as compared to the regular UTR 40 transformer oil coolant. Thus, transformers with reduced dimensions and higher efficiency with loading capacity and extended life duration may be designed.

http://dx.doi.org/10.5772/65556

5. Nanofluid with colloidal magnetic Fe_3O_4 nanoparticles used in microactuation process

Based on the afore described magnetic nanofluid, we can make a microactuator whose operation complies with the principle of Pulse Width Modulation (PWM) [23, 68]. The output PWM rectangular pulse form for a pulse duty factor of 14% is presented in **Figure 22**. The PWM generator discharges on the microactuator magnetic nanofluid impedances, two windings L_1 and L_2 (**Figure 23**). The electromagnetic force developed by the microactuator and implicitly the movement of the magnetic nanofluid depends mainly on the windings excitation voltage pulse duty factor *K*u %. Passing an electric current by the microactuator windings results a magnetic field. The net effect of this magnetic field is a mass transfer of the magnetic nanofluid.

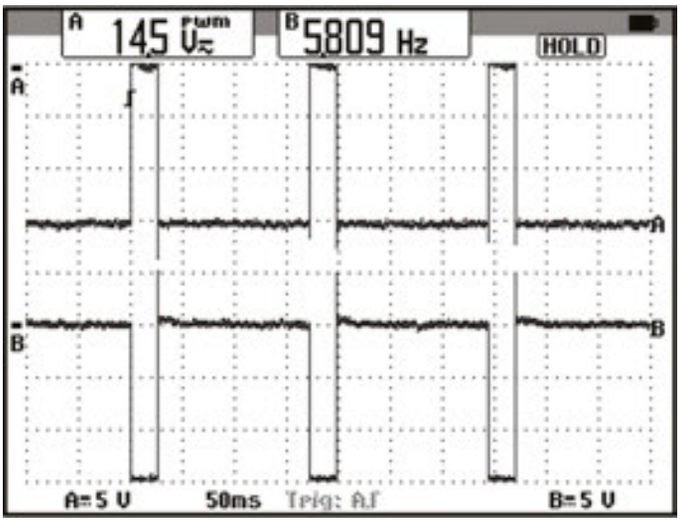

Figure 22. The output PWM rectangular pulse form, for a pulse duty factor of 14%.

Figure 23. The microactuator with magnetic nanofluid during testing [68].

Also, the maximum amplitude of the excitation voltage is constant, U_{max} = 15 V. The RMS value of the current that goes through the coils of the actuator, for a fixed frequency of the PWM voltage, depends mainly on the pulse duty factor. Two windings, L_1 and L_2, are excited with a rectangular waveform, counter phase, in compliance with **Figure 22**.

Acknowledgements

The authors express special thanks to Prof. Alexandru Mihail Morega, corresponding Member of the Romanian Academy, for valuable results concerning the numerical simulations. The research was performed with the support of UEFISCDI, PNCDI II Programme—Joint Applied Research Projects, Romania, Contract 63/2014, Environment energy harvesting hybrid system by photovoltaic and piezoelectric conversion, DC/DC transformation with MEMS integration and adaptive storage. Also, the numerical simulations were conducted in the Laboratory for Multiphysics Modeling, at UPB, with the support of the PNCDI-II "Parteneriate" Contract 21-043/2008.

Nomenclature

D (nm)	crystallites medium size
λ (nm)	wavelength of the Cu-Kα radiation (0.154059 nm)
B* (rad)	full width at half maximum (FWHM)
ϑ (^{o})	half diffraction angle of crystal orientation peak (Bragg angle)
M (A/m)	magnetization
M_r (A/m)	remnant magnetization
H_c (A/m)	coercive magnetic field
ρ (kg/m^3)	mass density
$\varphi_{Fe_3O_4}$ (-)	solid volume fraction of the dispersed magnetite
M_d (A/m)	monodomenial magnetization of magnetite (480 kA/m)
ξ (-)	Langevin parameter
L(ξ)=cothξ-1/ξ (-)	Langevin function
μ_0 (H/m)	magnetic permeability of vacuum ($4\pi \times 10^{-7}$ H/m)
μ (H/m)	magnetic permeability of the medium
μ_r (-)	relative magnetic permeability (μ/μ_0)
D_m (nm)	magnetic diameter
H (A/m)	magnetic field strength
k_B (J/K)	Boltzmann constant (1.38×10^{-23} J/K)
T (K)	absolute temperature
χ_{iL} (-)	initial magnetic susceptibility
M_S (A/m)	saturation magnetization
$\varphi_m = M_S/M_d$ (-)	magnetic volume fraction
f(x) (-)	log-normal distribution function

http://dx.doi.org/10.5772/65556

x (nm)	magnetic diameter of the magnetite particles – argument of the log-normal distribution function
f(x)dx (-)	probability that the magnetic diameter of the magnetic particles to be in the range of $(x;\ x + dx)$
D_0 (nm)	dimensional distribution parameter, defined by $\ln(D_0) = \langle \ln(x) \rangle$
S (-)	dimensional distribution parameter, representing the deviation of ln(x) value from $\ln(D_0)$
n (partic./m^3)	density of the dispersed magnetite particles
m (A m^2)	dipolar magnetic moment
σ (nm)	standard deviation
H_0 (A/m)	magnetic field strength, representing the ration of the magnetization curve slope and saturation magnetization, in M = f(1/H) representation
R^2 (-)	measure of accuracy of the fit in linear regression
δ_m (nm)	thickness of non-magnetic layer
D_p (nm)	physical (geometrical) diameter
δ_s (nm)	surfactant cover thickness
D_h (nm)	hydrodynamic diameter
$\dot{\gamma}$ (s^{-1})	shear rate
η (Pa s)	dynamic viscosity
η_{ref} (Pa s)	dynamic viscosity corresponding to the reference temperature, T_{ref}
T_{ref} (K)	reference temperature
E_a (J/mol)	activation energy
R (J/mol K)	ideal gas constant (8.31447 J/mol K)
k (W/m K)	thermal conductivity
k_e (W/m K)	effective thermal conductivity of the magnetic nanofluid
k_p (W/m K)	thermal conductivity of the magnetite nanoparticles
k_f (W/m K)	thermal conductivity of the carrier fluid
φ_e (-)	equivalent volume fraction
$\delta = 2\delta_m$ (nm)	double thickness of non-magnetic layer
u (-)	magnetic diameter dependent function
c_p (J/kg K)	specific heat at constant pressure
$c_{p,MNF}$ (J/kg K)	specific heat of the magnetic nanofluid
$c_{p,UTR}$ (J/kg K)	specific heat of the transformer oil
$c_{p,NP}$ (J/kg K)	specific heat of the magnetite nanoparticles
ρ_{MNF} (kg/m^3)	mass density of the magnetic fluid (0.960 g/cm^3, at 24°C)
ρ_{UTR} (kg/m^3)	mass density of the transformer oil (0.867 g/cm^3, at 20°C)
ρ_{NP} (kg/m^3)	mass density of the magnetite nanoparticles
β (1/K)	thermal expansion coefficient
β_{MNF} (1/K)	thermal expansion coefficient of the magnetic nanofluid
β_{UTR} (1/K)	thermal expansion coefficient of the transformer oil
β_{NP} (1/K)	thermal expansion coefficient of the magnetite nanoparticles
FOM_{NC} (-)	figure-of-merit determined for natural convection

n (-)	constant whose value depends on flow type; $n = 0.25$ for laminar flow and $n = 0.33$ for turbulent flow
ε (F/m)	electric permittivity
ε_0 (F/m)	electric permittivity of free space ($8.8541878176 \times 10^{-12}$ F/m)
ε_r (-)	relative electric permittivity ($\varepsilon_r = \varepsilon/\varepsilon_0$)
ε_{MNF} (F/m)	effective electric permittivity of the magnetic fluid
ε_{UTR} (F/m)	electric permittivity of the transformer oil
ε_{NP} (F/m)	electric permittivity of the magnetite nanoparticles
u (m/s)	velocity
ω (rad/s)	angular speed
p (N/m^2)	pressure
A (-)	magnetic vector field
E (V/m)	electric field strength
J_{φ}^{e} (A/m^2)	angular component of the current density
f_T (N)	buoyancy body force term
f_{mg} (N)	magnetic body force term
σ (S/m)	electrical conductivity
μ_f (m^2/s)	kinematics viscosity
B (T)	magnetic field induction
B_r (T)	remnant induction
a (A/m)	empiric constant (10^4 A/m)
b (m/A)	empiric constant (3×10^{-5} m/A)
T_{amb} (K)	ambient temperature (300 K)
h (W/m^2 K)	heat transfer coefficient
U_{max} (V)	excitation voltage at maximum amplitude

Author details

Lucian Pîslaru-Dănescu[1]*, Gabriela Telipan[1], Floriana D. Stoian[2], Sorin Holotescu[2] and Oana Maria Marinică[2]

*Address all correspondence to: lucian.pislaru@icpe-ca.ro

1 National Institute for Electrical Engineering ICPE-CA, Bucharest, Romania

2 Politehnica University of Timisoara, Timisoara, Romania

References

[1] Vékás L, Bica D, Avdeev M. Magnetic nanoparticles and concentrated magnetic nanofluids: Synthesis, properties and some applications. China Particuology. 2007;**5**(1–2):43–49.

[2] Ervithayasuporn V, Kawakawi Y. Synthesis and characterization of core-shell type Fe_3O_4 nanoparticles in poly (organosilsesquixane). Journal of Colloid and Interface Science. 2009;**332**:389–393. DOI: 10.1016/j.jcis.2008.12.061

[3] Gubin S P. Magnetic Nanoparticles. Wiley - VCH Verlag Gmb H&Co. Weinheim, Germany; 2009. 466 p. DOI: 10.1002/9783527627561

[4] Vékás L, Bica D, Marinica O. Magnetic nanofluid stabilized with various chain length surfactants. Romanian Reports in Physics. 2006;**58**(3):257–267.

[5] Arulmurugan R, Vaidyanathan G, Sendhilnathan S, Jeyadevan B. Mn-Zn ferrite nanoparticles for ferrofluid preparation: Study on thermal-magnetic properties. Journal of Magnetism and Magnetic Materials. 2006;**298**(2):83–94.

[6] Hayashi K, Sakamoto W, Yogo T. Magnetic and rheological properties of monodisperse Fe_3O_4 nanoparticles/organic hybrid. Journal of Magnetism and Magnetic Materials. 2009;**321**:450–457. DOI: 10.1016/j.jmmm.2008.10.004

[7] Gupta A K, Gupta M. Synthesis and surface engineering of iron oxide nanoparticles. Biomaterials. 2005;**26**:3995–4021. DOI: 10.1016/j.biomaterials.2004.10.012

[8] Ozkaya T, Toprak M S, Baykal A, Kavas H, Koseoglu Y, Aktas B. Synthesis of Fe_3O_4 nanoparticles at 100°C and its magnetic characterization. Journal of Alloys and Compounds. 2009;**472**:18–23. DOI: 10.1016/j.jallcom.2008.04.101

[9] Paddar P, Fried T, Markovich G, Sharoni A, Katz D, Wizansky T, Mills O. Manifestation of the Verwey transition in the tunneling spectra of magnetite nanocrystals. Europhysics Letters. 2003;**64**(1):98–103. DOI: 10.1209/epl/i2003-00141-0

[10] Jordan K, Cazacu A, Manai G, Ceballos S F, Murphy S, Shvets I V. Scanning tunneling spectroscopy study of the electronic structure of Fe_3O_4 surfaces. Physical Review. 2006;**74**:085416. DOI: 10.1103/PhysRevB.74.085416

[11] Chastellain M, Petri A, Hofmann H. Particles size investigations of a multistep synthesis of PVA coated superparamagnetic nanoparticles. Journal of Colloid and Interface Science. 2004;**278**:353–360. DOI: 10.1016/j.jcis.2004.06.025

[12] Marques R F C, Garcia C, Lecante P, Ribeiro S J L, Noe L, Silva N J O, Amaral V S, Millan A, Verelst M. Electro-precipitation of Fe_3O_4 nanoparticles in ethanol. Journal of Magnetism and Magnetic Materials. 2008;**320**:2311–2315. DOI: 10.1016/j.jmmm.2008.04.165

[13] Abu Mukh-Qasem R, Gedanken A. Sonochemical synthesis of stable hydrosol of Fe_3O_4 nanoparticles. Journal of Colloid and Interface Science. 2005;**284**:489–494. DOI: 10.1016/j.jcis.2004.10.073

[14] Cai Y, Shen Y, Xie A, Li S, Wang X. Green synthesis of soya bean sprouts-mediated superparamagnetic Fe_3O_4 nanoparticles. Journal of Magnetism and Magnetic Materials. 2010;**322**:2938–2943. DOI: 10.1016/j.jmmm.2010.05.009

[15] Cabrera L, Gutierrez S, Menendez N, Morales M P, Herrasti P. Magnetite nanoparticles: Electrochemical synthesis and characterization. Electrochimica Acta. 2008;**53**:3436–3441. DOI: 10.1016/j.electacta.2007.12.006

[16] Neuberger T, Schöpf B, Hofmann H, Hofmann M, von Rechenberg B. Superparamagnetic nanoparticles for biomedical applications: Possibilities and limitations of a new drug delivery system. Journal of Magnetism and Magnetic Materials. 2005;**293**:483–496. DOI: 10.1016/j.jmmm.2005.01.064

[17] Maity D, Agrawal D C. Synthesis of iron oxide nanoparticles under oxidizing environment and their stabilization in aqueous and non-aqueous media. Journal of Magnetism and Magnetic Materials. 2007;**308**:46–55. DOI: 10.1016/j.jmmm.2006.05.001

[18] Park G S, Park S H. Design of magnetic fluid linear pump. IEEE Transactions on Magnetics. 1999;**35**:4058–4060. DOI: 10.1109/20.800754

[19] Park G S, Seo K. New design of the magnetic fluid linear pump to reduce the discontinuities of the pumping forces. IEEE Transactions on Magnetics. 2004;**40**(2):916–919. DOI: 10.1109/TMAG.2004.824718

[20] Nethe A, Scholz T, Stahlmann H-D, Filtz M. Ferrofluids in electric motors: A numerical process model. IEEE Transactions on Magnetics. 2002;**38**(2):1177–1180. DOI: 10.1109/20.996301

[21] Choi I H, Hong S P, Chung W E, Kim Y J, Lee M H, Kim J Y. Concentrated anisotropic magnetization for high sensitivity of optical pickup actuator. IEEE Transactions on Magnetics. 1999;**35**(3):1861–1864. DOI: 10.1109/20.767396

[22] Ahn J J, Oh J G, Choi B. A study of the novel type of ferrofluid magnetic pipette. In Nanotech – Technical Proceedings of the 2003 Nanotechnology Conference and Trade Show; 23–27 February 2003; San Francisco. Cambridge, MA: Nano Science and Technology Institute; 2003. p. 226–229.

[23] Pîslaru-Dănescu L, Morega A M, Telipan G, Stoica V. Nanoparticles of ferrofluid Fe_3O_4 synthetised by coprecipitation method used in microactuation process. Optoelectronics and Advanced Materials—Rapid Communications. 2010;**4**(8):1182–1186. WOS:000281734800030

[24] Turcu R, Craciunescu I, Nan A. Magnetic Microgels: Synthesis and Characterization. In Nirschl H, Keller K, Eds., Upscaling of Bio-Nano-Processes: Selective Bioseparation by Magnetic Particles. Springer-Verlag, Berlin Heidelberg, Germany. 2014; p. 57–76.

[25] Nkurikiyimfura I, Wang Y, Pan Z. Heat transfer enhancement by magnetic nanofluids: A review. Renewable and Sustainable Energy Reviews. 2013;**21**:548–561. DOI: 10.1016/j.rser.2012.12.039

[26] Sheikholeslami M, Ganji D D. Ferrohydrodynamic and magnetohydrodynamic effects on ferrofluid flow and convective heat transfer. Energy. 2014;**75**:400–410. DOI: 10.1016/j.energy.2014.07.089

[27] Sheikholeslami M, Rashidi M M, Ganji D D. Numerical investigation of magnetic nanofluid forced convective heat transfer in existence of variable magnetic field using two phase model. Journal of Molecular Liquids. 2015;**212**:117–126. DOI: 10.1016/j.molliq.2015.07.077

[28] Patel J, Parekh K, Upadhyay R V. Prevention of hot spot temperature in a distribution transformer using magnetic fluid as coolant. International Journal of Thermal Sciences. 2016;**103**:35–40.

[29] Sheikholeslami M, Hayat T, Alsaedi A. MHD free convection of Al2O3–water nanofluid considering thermal radiation: A numerical study. International Journal of Heat and Mass Transfer. 2016;**96**:513–524. DOI: 10.1016/j.ijheatmasstransfer.2016.01.059

[30] Tsai T-H, Kuo L-S, Chen P H, Lee D-S, Yang C-T. Applications of ferro-nanofluid on a micro-transformer. Sensors. 2010;**10**:8161–8172.

[31] Dumitru J B, Morega A M, Pîslaru-Dănescu L, Morega M. A parametric study of lumped circuit parameters of a miniature planar spiral transformer. In Proceedings of the Advanced Topics in Electrical Engineering (ATEE), 8th International Symposium; 23–25 May 2013; Bucharest, Romania. IEEEXplore Digital Library, US; 2013. DOI: 10.1109/ATEE.2013.6563477

[32] Shliomis M I. Magnetic fluids. Soviet Physics Uspekhi. 1974;**17**(3):153–169. DOI: 10.1070/PU1974v017n02ABEH004332

[33] Rosensweig R E. Ferrohydrodynamics. Journal of Applied Mathematics and Mechanics. 1986;**67**(6):279. DOI: 10.1002/zamm.19870670626

[34] Chantrell R W, Popplewell J, Charles S W. Measurements particle size distribution parameters in ferrofluids. IEEE Transactions on Magnetics. 1978;**14**:975–977. DOI: 10.1109/TMAG.1978.1059918

[35] Cogoni G, Grosso M, Baratti R, Romagnoli J A. Time evolution of the PSD in crystallization operations: An analytical solution based on Ornstein-Uhlenbeck process. AIChE Journal. 2012;**58**(12):3731–3739. DOI: 10.1002/aic.13760

[36] Susan-Resiga D, Socoliuc V, Boros T, Borbáth T, Marinica O, Han A, Vekas L. The influence of particle clustering on the rheological properties of highly concentrated magnetic nanofluids. Journal of Colloid and Interface Science. 2012;**373**:110–115. DOI: 10.1016/j.jcis.2011.10.060

[37] Ivanov A O. Magnetostatic properties of moderately concentrated ferrocolloids. Magnitnaia Gidrodinamika. 1992;**28**(4):39–46.

[38] Pshenichnikov A F, Mekhonoshin W V, Lebedev A V. Magneto-granulometric analysis of concentrated ferrocolloids. Journal of Magnetism and Magnetic Materials. 1996;**161**:94–102. DOI: 10.1016/S0304-8853(96)00067-4

[39] Raj K, Moskowitz R. Ferrofluid-cooled electromagnetic device and improved cooling method. US Patent 5462685. 1995.

[40] Kader T, Bernstein S, Crowe C. Magnetic fluid cooler transformer. US Patent 5898353 A. 1997.

[41] Pîslaru-Dănescu L, Macamete E, Telipan G, Pintea J, Nouras F, Paduraru N, Vekas L, Stoian F, Borbath I, Borbath T, Morega A, Morega M. Transformer with magnetic nanofluid as cooling agent. RO Patent 126613 B1. 2011.

[42] Segal V, Rabinovich A, Nattrass D, Raj K, Nunes A. Experimental study of magnetic colloidal fluids behavior in power transformers. Journal of Magnetism and Magnetic Materials. 2000;**215–216**:513–515. DOI: 10.1016/S0304-8853(00)00205-5

[43] Morega A M, Morega M, Pîslaru-Dănescu L, Stoica V, Nouraş F, Stoian F D. A novel, ferrofluid-cooled transformer. Electromagnetic field and heat transfer by numerical simulation. In Proceedings of the 12th International Conference on Optimization of Electrical and Electronic Equipment (OPTIM 2010); 20–22 May 2010; Brasov, Romania. IEEEXplore Digital Library, US; 2010. p. 140–146. DOI: 10.1109/OPTIM.2010.5510425

[44] Pîslaru-Dănescu L, Morega A M, Morega M, Stoica V, Marinica O, Nouraş F, Paduraru N, Borbath I, Borbath T. Prototyping a ferrofluid-cooled transformer. IEEE Transactions on Industry Applications. 2012;**49(**3):1289–1298. DOI: 10.1109/TIA.2013.2252872

[45] Stoian F D, Holotescu S, Taculescu A, Marinica O, Susan-Resiga D, Timko M, Kopcansky P, Rajnak M. Characteristic properties of a magnetic nanofluid used as cooling and insulating medium in a power transformer. In Proceedings of the 8th International Symposium on Advanced Topics in Electrical Engineering (ATEE); 23–25 May 2013; Bucharest, Romania. IEEEXplore Digital Library, US; 2013. p. 1–4. DOI: 10.1109/ATEE.2013.6563463

[46] Ostoja-Starzewski M. Microstructural randomness versus representative volume element in thermomechanics. ASME Journal of Applied Mechanics. 2002;**69**:25–35. DOI: 10.1115/1.1410366

[47] Torquato S. Random Heterogeneous Materials. Springer-Verlag: New York; 2002. 703 p. DOI: 10.1007/978-1-4757-6355-3

[48] Yu W, France D M, Routbort J L, Choi S U S. Review and comparison of nanofluid thermal conductivity and heat transfer enhancements. Heat Transfer Engineering. 2008;**29**(5):432–460. DOI: 10.1080/01457630701850851

[49] Timko M, Kopcansky P, Molcan M, Tomco L, Marton K, Molokac S, Rybar P, Stoian F D, Holotescu S, Taculescu A. Magnetodielectric properties of transformer oil based magnetic fluids. Acta Physica Polonica A. 2012;**121**(5–6):1253–1256. DOI: 10.12693/APhysPolA.121.1253

[50] Timko M, Marton K, Tomco L, Kiraly J, Molcan M, Rajnak M, Kopcansky P, Cimbala R, Stoian F D, Holotescu S, Taculescu A. Magneto-dielectric properties of transformer oil based magnetic fluids in the frequency range up to 2 MHz. Magnetohydrodynamics. 2012;**48**(2):427–434.

[51] Perrier C, Beroual A, Bessede J-L. Improvement of power transformers by using mixtures of mineral oil with synthetic esters. IEEE Transaction on Dielectrics and Electrical Insulation. 2006;**13**(5):556–564. DOI: 10.1109/TDEI.2006.1657968

[52] MIDEL. Specific heat – MIDEL 7131 – Specific Heat vs. Temperature [Internet]. Available from: http://www.midel.com/productsmidel/midel-7131/thermal-properties/specific-heat [Accessed: 2016-07-13].

[53] Wang H J, Ma S J, Yu H M, Zhang Q, Guo C M, Wang P. Thermal conductivity of transformer oil from 253 K to 363 K. Petroleum Science and Technology. 2014;**32**(17):2143–2150. DOI: 10.1080/10916466.2012.757235

[54] Philip J, Shima P D, Raj B. Enhancement of thermal conductivity in magnetite based nanofluid due to chainlike structures. Applied Physics Letters. 2007;**91**(20):203108. DOI: 10.1063/1.28126699

[55] Holotescu S, Stoian F D. A study of the influence of filler dimensional distribution on the polymer composite effective thermal conductivity. In Proceedings of the 29th Japan Symposium of Thermophysical Properties; 8–10 October 2008; Tokyo. Japan Society of Thermophysical Properties, Tokyo, Japan; 2008. p. 318–320

[56] Holotescu S, Stoian F D. Evaluation of the effective thermal conductivity for composite polymers by considering the filler size distribution law. Journal of Zhejiang University SCIENCE A. 2009;**10**:704–709. DOI: 10.1631/jzus.A0820733

[57] Holotescu S, Stoian F D, Marinica O, Kubicar L, Kopcansky P, Timko M. Utilization of the magnetogranulometric analysis to estimate the thermal conductivity of magnetic fluids. Journal of Magnetism and Magnetic Materials. 2011;**323**(10):1343–1347. DOI: 10.1016/j.jmmm.2010.11.043

[58] Khanafer K, Vafai K. A critical synthesis of thermophysical characteristics of nanofluids. International Journal of Heat and Mass Transfer. 2011;**54**:4410–4428. DOI: 10.1016/j.ijheatmasstransfer.2011.04.048

[59] Hopstock D M, Zanko L M. Minnesota taconite as a microwave-absorbing road aggregate material for deicing and pothole patching applications. Final Report, CTS Report No. 2004019. University of Minnesota, Duluth, US; 2005. 26 p.

[60] Korolev V V, Aref'ev I M, Ramazanova A G. Magnetocaloric effect and the heat capacity of ferrimagnetic nanosystems in magnetic fluids. Russian Journal of Physical Chemistry A. 2007;**81**(10):1677–1680. DOI: 10.1134/S003602440710024X

[61] Ravnik J, Skerget L, Hribersek M. Analysis of three-dimensional convection of nanofluids by BEM. Engineering Analysis with Boundary Elements. 2010;**34**:1018–1030. DOI: 10.1016/j.enganabound.2010.06.019

[62] Susa D, Lehtonen M, Nordman H. Dynamic modelling of power transformers. IEEE Transactions on Power Delivery. 2005;**20**(1):197–204. DOI: 10.1109/TPWRD.2004.835255

[63] Nikolaev V A, Shipilin A M. On the thermal expansion of nanoparticles. Physics of the Solid State. 2000;**42**(1):109–110. DOI: 10.1134/1.1131176

[64] Bergles A E, Bar-Cohen A. Immersion Cooling of Digital Computers, in Cooling of Electronic Systems. Publisher Springer Netherlands; NATO Advanced Study Institute Series; 1994. p. 539–621. Print ISBN 978-94-010-4476-9; Online ISBN 978-94-011-1090-7; Series ISSN 0168-132X; DOI: 10.1007/978-94-011-1090-7_23

[65] COMSOL MultiPhysics, Comsol A.B. Sweden, v. 3.5a (2010), v. 4.2a (2012), v 4.3 (2013). www.comsol.com

[66] Stoian F D, Holotescu S, Stoica V, Bica D, Vekas L. Comparative study of convective heat transfer in water and water based magnetizable nanofluid for thermal applications. Journal of Optoelectronics and Advanced Materials. 2008;**10**(4):773–776.

[67] Pîslaru-Dănescu L, Morega A M, Telipan G, Morega M, Dumitru J B, Marinescu V. Magnetic nanofluid applications in electrical engineering. IEEE Transactions on Magnetics. 2013;49(11):5489–5497. DOI: 10.1109/TMAG.2013.2271607

[68] Morega A M, Pîslaru-Dănescu L, Morega M. A novel microactuator device based on magnetic nanofluid. In: Proceedings of the 12th International Conference on Optimization of Electrical and Electronic Equipment (OPTIM 2012); 24–26 May 2012; Basov, Romania. IEEEXplore Digital Library, US; 2012. p. 1100–1106. DOI: 10.1109/OPTIM.2012.6231963